



University of Maribor

Faculty of Energy Technology

# Journal of ENERGY TECHNOLOGY



Volume 13 / Issue 1

MAY 2020

[www.fe.um.si/en/jet.html](http://www.fe.um.si/en/jet.html)



# Journal of ENERGY TECHNOLOGY



**VOLUME 13 / Issue 1**

Revija Journal of Energy Technology (JET) je indeksirana v bazah INSPEC© in Proquest's Technology Research Database.

The Journal of Energy Technology (JET) is indexed and abstracted in database INSPEC© and Proquest's Technology Research Database.



# JOURNAL OF ENERGY TECHNOLOGY

## Ustanovitelj / FOUNDER

Fakulteta za energetiko, UNIVERZA V MARIBORU /  
FACULTY OF ENERGY TECHNOLOGY, UNIVERSITY OF MARIBOR

## Izdajatelj / PUBLISHER

Fakulteta za energetiko, UNIVERZA V MARIBORU /  
FACULTY OF ENERGY TECHNOLOGY, UNIVERSITY OF MARIBOR

## Glavni in odgovorni urednik / EDITOR-IN-CHIEF

Jurij AVSEC

## Souredniki / CO-EDITORS

Bruno CVIKL  
Miralem HADŽISELIMOVIĆ  
Gorazd HREN  
Zdravko PRAUNSEIS  
Sebastijan SEME  
Bojan ŠTUMBERGER  
Janez USENIK  
Peter VIRTič  
Ivan ŽAGAR

## Uredniški odbor / EDITORIAL BOARD

**Dr. Anton BERGANT,**  
Litostroj Power d.d., Slovenia

**Prof. dr. Marinko BARUKČIĆ,**  
Josip Juraj Strossmayer University of Osijek, Croatia

**Prof. dr. Goga CVETKOVSKI,**  
Ss. Cyril and Methodius University in Skopje, Macedonia

**Prof. dr. Nenad CVETKOVIĆ,**  
University of Nis, Serbia

**Prof. ddr. Denis ĐONLAGIĆ,**  
University of Maribor, Slovenia

**Doc. dr. Brigita FERČEC,**  
University of Maribor, Slovenia

**Prof. dr. Željko HEDERIĆ,**  
Josip Juraj Strossmayer University of Osijek, Croatia

**Prof. dr. Marko JESENIK,**  
University of Maribor, Slovenia

**Prof. dr. Ivan Aleksander KODELI,**  
Jožef Stefan Institute, Slovenia

**Prof. dr. Rebeka KOVAČIČ LUKMAN,**  
University of Maribor, Slovenia

**Prof. dr. Milan MARČIČ,**  
University of Maribor, Slovenia

**Prof. dr. Igor MEDVED,**  
Slovak University of Technology in Bratislava, Slovakia

**Prof. dr. Matej MENCINGER,**  
University of Maribor, Slovenia

**Prof. dr. Greg NATERER,**  
Memorial University of Newfoundland, Canada

**Prof. dr. Enrico NOBILE,**  
University of Trieste, Italia

**Prof. dr. Urška LAVRENČIČ ŠTANGAR,**  
University of Ljubljana, Slovenia

**Doc. dr. Luka SNOJ,**  
Jožef Stefan Institute, Slovenia

**Prof. Simon ŠPACAPAN,**  
University of Maribor, Slovenia

**Prof. dr. Gorazd ŠTUMBERGER,**  
University of Maribor, Slovenia

**Prof. dr. Anton TRNIK,**  
Constantine the Philosopher University in Nitra, Slovakia

**Prof. dr. Zdravko VIRAG,**  
University of Zagreb, Croatia

**Prof. dr. Mykhailo ZAGIRNYAK,**  
Kremenchuk Mykhailo Ostrohradskiy National University, Ukraine

**Prof. dr. Marija ŽIVIĆ,**  
Josip Juraj Strossmayer University of Osijek, Croatia

**Tehnični urednik / TECHNICAL EDITOR**

Sonja Novak

**Tehnična podpora / TECHNICAL SUPPORT**

Tamara BREČKO BOGOVČIČ

**Izhajanje revije / PUBLISHING**

Revija izhaja štirikrat letno v nakladi 100 izvodov. Članki so dostopni na spletni strani revije - [www.fe.um.si/si/jet.html](http://www.fe.um.si/si/jet.html) / The journal is published four times a year. Articles are available at the journal's home page - [www.fe.um.si/en/jet.html](http://www.fe.um.si/en/jet.html).

Cena posameznega izvoda revije (brez DDV) / Price per issue (VAT not included in price): 50,00 EUR

Informacije o naročninah / Subscription information: <http://www.fe.um.si/en/jet/subscriptions.html>

**Lektoriranje / LANGUAGE EDITING**

Terry T. JACKSON

**Oblikovanje in tisk / DESIGN AND PRINT**

Fotografika, Boštjan Colarič s.p.

**Naslovna fotografija / COVER PHOTOGRAPH**

Jurij AVSEC

**Oblikovanje znaka revije / JOURNAL AND LOGO DESIGN**

Andrej PREDIN

**Ustanovni urednik / FOUNDING EDITOR**

Andrej PREDIN

## ***Spoštovani bralci revije Journal of energy technology (JET)***

Razvoj novih materialov je za energetiko izjemnega pomena. Novi materiali omogočajo boljšo učinkovitost, izboljšujejo lastnosti naprav, podaljšujejo njihovo življenjsko dobo. Z razvojem novih materialov se na primer izboljšuje tudi učinkovitost fotovoltaičnih modulov, povečujeta se moč in življenjska doba baterij. Število novo odkritih materialov je ogromno, po nekaterih podatkih jih je več milijonov. Zmesi je neprimerno več. Za vsak material je potrebno poznati vsaj 15 termomehanskih lastnosti v območju temeperatur in tlakov. Za določitev termomehanskih lastnosti čistih materialov in njihovih zmesi je potrebno izvesti eksperimente, ali s pomočjo matematično-fizikalnih modelov izračunati lastnosti, kar seveda v vsakem primeru zahteva veliko časa in finančnih sredstev. Do zdaj je raziskan in v revijah objavljen le manjši del odkritih materialov oz. zmesi, zato je vsak prispevek o novih odkritjih s tega področja izjemnega pomena. V tej številki objavljamo prispevek k širjenju odkritij v materialih.

Jurij AVSEC  
odgovorni urednik revije JET

## ***Dear Readers of the Journal of Energy Technology (JET)***

The science of developing new materials is essential to energy engineering. New materials enable greater efficiency and improve both the performance and lifespan of devices. For example, the development of new materials improves the efficiency of photovoltaic modules and increases the power and battery lifespan. There is a massive number of materials in the world, (millions, even) and multiple mixtures of each of them. For each material, it is necessary to know at least 15 thermomechanical properties regarding temperatures and pressures. To determine the thermomechanical properties of pure materials and their mixtures, it is necessary to perform very expensive experiments (which requires an enormous amount of time too) or to calculate the properties with the help of mathematical-physical models, which (of course) requires much time and financial resources. Thus far, only a small amount of discovered materials or mixtures have been researched and the subsequent findings published in journals. Therefore, any contribution to new discoveries in the field of materials is extremely important. This issue of JET contributes to this knowledge.

Jurij AVSEC  
Editor-in-chief of JET

# ***Table of Contents / Kazalo***

## **The influence of delta ferrite on the quality assessment of austenitic stainless steel welds for the production of ovens**

Vpliv delta ferita na kakovost avstenitnih nerjavnih zvarov za proizvodnjo pečic

**Zdravko Praunseis . . . . . 11**

## **Impacts of zero-emission powertrains based on hydrogen technologies in public transport**

Vplivi uporabe nizko-emisijskih pogonskih sklopov na podlagi vodikovih tehnologij v javnem transportu

**Niko Natek, Boštjan Krajnc . . . . . 25**

## **A simplified hybrid methodology for designing coreless axial flux machines**

Poenostavljena metoda za načrtovanje sinhronskih strojev s trajnimi magneti in aksialnim magnetnim pretokom brez feromagnetnega jedra statorja

**Franjo Pranjč, Peter Vrtič . . . . . 39**

## **Improving decentralized economic growth and reducing energy consumption with the application of ecologically oriented innovations**

Izboljšanje decentralizirane gospodarske rasti v Evropski uniji in zmanjševanje rabe energije z uporabo ekološko naravnanih inovacij

**Niko Natek, Boštjan Krajnc . . . . . 55**

**Instructions for authors . . . . . 63**

# THE INFLUENCE OF DELTA FERRITE ON THE QUALITY ASSESSMENT OF AUSTENITIC STAINLESS STEEL WELDS FOR THE PRODUCTION OF OVENS

## VPLIV DELTA FERITA NA KAKOVOST AVSTENITNIH NERJAVNIH ZVAROV ZA PROIZVODNJO PEČIČ

Zdravko Praunseis<sup>31</sup>

**Keywords:** austenitic stainless steel, delta ferrite, quality assessment, welded joints, production of ovens

### **Abstract**

Rust-resistant metals, such as the popular stainless steel, often contain some quantities of delta ( $\delta$ ) ferrite that lower the mechanical properties of welded joints. The results of the study show that the amount of  $\delta$ -ferrite influences the quality assessment of austenitic stainless steel welds for the production of ovens using the resistance seam welding process.

In this article, the basic device of resistance seam welding for the production of stainless steel welds is described. The device itself will have a significant role in the operation of the line; therefore, it was very precisely constructed and designed.

### **Povzetek**

Nerjavne kovine, kot je poznano nerjavno jeklo, pogostokrat vsebuje določene količine delta ferita ( $\delta$ ), ki znižuje mehanske lastnosti zvarnih spojev. Rezultati študije kažejo na to, da vsebnost delta ferita vpliva na kakovost zvarov zgrajenih iz avstenitnih nerjavnih jekel za proizvodnjo pečic z uporovnim točkovnim varilnim procesom.

<sup>31</sup> Corresponding author: Associate Professor, Zdravko Praunseis, PhD, Faculty of Energy Technology, University of Maribor, Tel.: +386 31 743 753, Hočevarjev trg 1, Krško, Slovenia, E-mail address: [zdravko.praunseis@um.si](mailto:zdravko.praunseis@um.si)

V članku je predstavljena osnovna varilna naprava za izgradnjo nerjavnih jeklenih zvarov s pomočjo točkovnega uporabnega varjenja. Naprava ima pomembno vlogo v proizvodnji liniji pečic in je zato natančno skonstruirana in oblikovana.

## 1 INTRODUCTION

Delta ferrite content in stainless steels is limited by international standards and is an important step in the manufacturing process of many types of industrial equipment. It is well known that the content of delta ferrite strongly affects the project's life-span prediction, hot cracking, stress corrosion cracking and solidification cracking. The expected value of ferrite content in the weld material is from 2 to 5%.

Delta ferrite microstructures in stainless steel and welded joints are determined by optical microscopy, scanning electron microscopy, X-ray diffraction, metallographic replication, vibrating sample magnetometer, as well as by the ferritoscopes, which is the most useful technique for delta ferrite measuring. Because of its portability, the equipment is simple to operate and provides a direct non-destructive response for different types of stainless steels. A standard calibration test with calibration samples made from austenitic, duplex and superduplex stainless steel should be carried out before experimental measurement with the ferritoscope. The calibration samples are correlated with the ferritoscope's magnetic response, and a specific calibration curve is configured in the equipment, [1-4].

The present research work made a careful experimental analysis of the ferrite content results achieved with the ferritoscope and presents a proper selection of austenitic stainless steel for the production of ovens using the resistance seam welding process, [7].

## 2 EXPERIMENTAL PROCEDURE AND RESULTS

Delta ferrite in austenitic stainless steel welds increases resistance to stress corrosion cracking (SCC). The effect is similar to the beneficial effect of increasing ferrite phase content in duplex stainless steels. In the welds of austenitic stainless steels, [4], the presence of fine, isolated pools of ferrite force the propagating crack to take a convoluted path, increasing its resistance to SCC. The effect of low-temperature thermal ageing (simulating the long-term exposure of the welds to the operating temperature of the nuclear reactors) on SCC in a high-temperature aqueous environment has suggested, [1-3], that the threshold stress level for SCC initiation was lower for the austenite-to-ferrite mode of solidification weld as compared to that for the ferrite-to-the austenite solidification mode weld (for type 316L stainless steel). Since the ferrite phase solidified in the austenite-to-ferrite mode had a higher chromium content, it was suggested that it might have a higher resistance to SCC than the weld that solidified in the ferrite-to-austenite mode. The ferrite content was calibrated and measured with a Fisher device ferritoscope, as shown in Figures 1, 2, and 3.



**Figure 1:** Calibrating of ferritoscope device Fisher with calibration samples, [5]



**Figure 2:** Non-destructive measuring of delta ferrite content in austenitic welds with ferritoscope device Fisher, [5]

Between the austenite and  $\delta$ -ferrite phase fields, there is a restricted ( $\alpha$ + $\gamma$ ) region that can be used to obtain two-phase or duplex structures in stainless steels. The structures are produced by having the correct balance between the  $\alpha$ -forming elements (Mo, Ti, Nb, Si, and Al) and the  $\gamma$ -forming elements (Ni, Mn, C, and N). To achieve a duplex structure, it normally is necessary to increase the chromium content to above 20 wt%. However, the exact proportions of  $\alpha$  and  $\gamma$  are determined by the heat treatment. It is clear from the consideration of the  $\gamma$ -loop section of the equilibrium diagram that holding in the range 1000–1300 °C will cause the ferrite content to vary over wide limits. The usual treatment is carried out between 1050 °C and 1150 °C, when the ferrite content is not sensitive to the subsequent cooling rate.

Duplex steels are stronger than the simple austenitic steels, partly as a result of the two-phase structure and also because this normally leads to a refinement of the grain size. Indeed, with suitable thermomechanical treatment between 900 °C and 1000 °C, it is possible to obtain very fine microduplex structures that can exhibit super-plasticity, i.e., very high ductilities at high temperatures, for strain rates less than a critical value. A further advantage is that duplex stainless steels are resistant to *solidification* cracking, particularly that which is associated with welding.

While the presence of  $\delta$ -ferrite may have an adverse effect on corrosion resistance in some circumstances, it does improve the resistance of the steel to transgranular stress corrosion cracking as the ferrite phase is immune to this type of failure.

The super-duplex stainless steels have even better corrosion resistance than the duplex stainless steels. They are particularly superior in their resistance to localised pitting corrosion [1-4], because of their larger concentrations of chromium, molybdenum and nitrogen. To maintain the balanced ferrite/austenite microstructure, it is also necessary to boost the concentration of austenite stabilising elements, such as nickel. Super-duplex stainless steels, therefore, typically contain 27Cr-7Ni-4Mo-0.3N wt%.

Another important group of stainless steels is essentially ferritic in structure and contains between 10 and 30 wt% chromium and, by dispensing with the austenite stabilising element nickel, possesses a considerable economic advantage. These steels, particularly at the higher chromium levels, have excellent corrosion resistance in many environments and are completely free from stress corrosion. For some applications, such as the exhaust system of a car, the chromium concentration can be limited because this provides sufficient corrosion and oxidation resistance while at the same time making the alloy formable; ferrite also has a much lower thermal expansion coefficient than austenite, so that fatigue induced by temperature variation can be mitigated. The ferritic stainless steels are somewhat stronger than austenitic stainless steels, the yield stresses being in the range 300–400 MPa, but they work harden less so the tensile strengths are similar, being between 500 and 600 MPa. However, ferritic stainless steels, in general, are not as readily deep-drawn as austenitic alloys because of the overall lower ductility. However, they are suitable for other deformation processes such as spinning and cold forging, [1-4].

Welding causes problems due to excessive grain growth in the heat-affected zone but, recently, new low-interstitial alloys containing titanium or niobium have been shown to be readily weldable. The higher chromium ferritic alloys have excellent corrosion resistance, particularly if 1–2 wt% molybdenum is present.

Two phenomena may adversely affect the behaviour of ferritic stainless steels. First, chromium-rich ferrites when heated between 400°C and 500°C develop a type of embrittlement, typically known as the 475°C embrittlement.

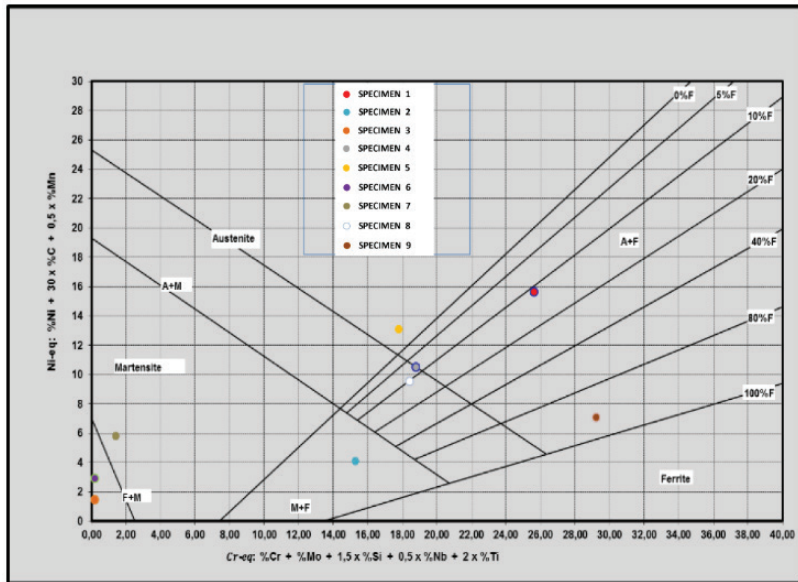


Figure 3: Measured delta ferrite content in nine specimens of austenitic stainless steel, [5]

Welding is implemented on two joints, where the plates of U-circumference and the ceiling overlap by a few millimetres, (Figure 4), [6-7].

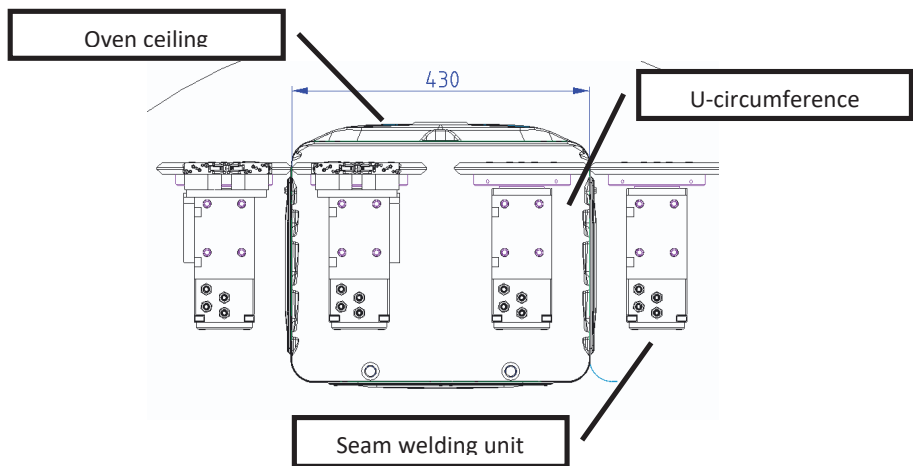


Figure 4: Welding sketch, [7]

Ceilings are taken from a specially modified transporter with a robot arm with a pneumatic gripper, and they are additionally positioned on a special unit in the X,Y directions.

Ceilings are then delivered to a rotatable unit, where they are positioned on lateral stands and vacuum-clamped. The U-circumference is loaded with a line manipulator (two-dimensional manipulator with several sequential grippers). The robot transfers the U-circumferences with a pneumatic gripper from a U-bending station to a line manipulator entry place (Figure 5), [7].

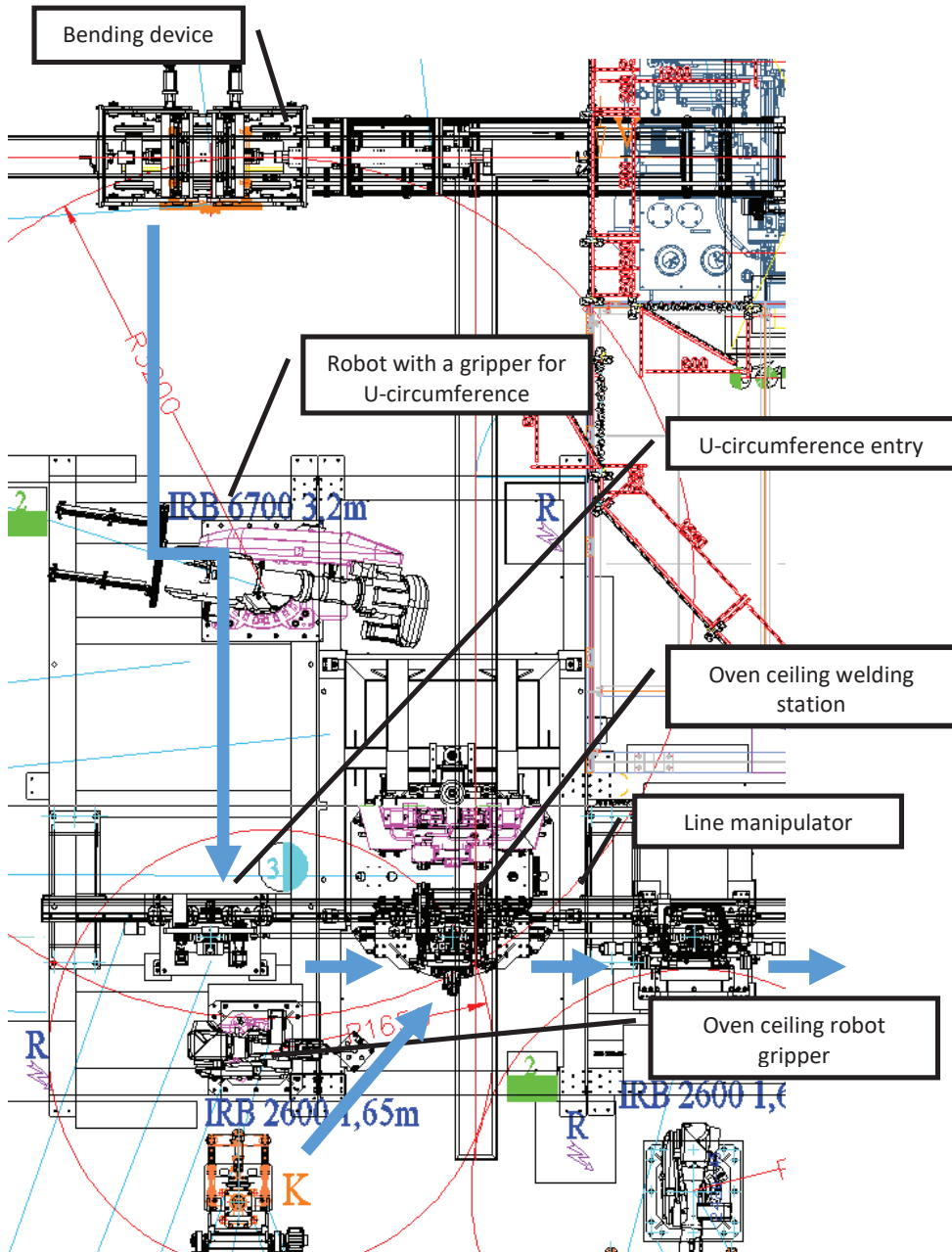


Figure 5: Station's ground plan [7]

The line consists of four main connecting segments:

- U-circumference formation,
- composing and welding of the oven,
- manufacturing the oven's back end,
- transport system.

There is an unwinding station with a lifting unit for a sheet reel at the beginning of the line. After the straightening and cutting station is the station for storing cut sheets, which ensures smooth line functioning during the sheet reel exchanges.

After that, there is a station for the lubrication of cut sheets and a serving unit that transfers the sheets further in the presses, which contains hole-cutting tools, and after that on a conveyor. The U-bending station is at the end.

The robot is transmitting the U-circumference with a gripper on a composition and welding part of the line. The main feature of that part of the line is a line manipulator with 14 grippers, which are transferring ovens from one station to the other at the same time. In this part of the line, there are stations for welding and shaping different oven assembly parts. At the end of that part of the line, the carriers for enamelling are welded. At the very end of the welding line, there is a unit for the automatic assembly and welding of the oven and front end, where the robot with a pneumatic gripper is transferring the front ends from a line storage container. A set of stations for manufacturing of the back ends serves for the production of many variants of cut back ends and shapes. Back ends are delivered from line storage transporters and a robot with a pneumatic gripper on to a welding station. Custom-designed welding units are spot welding the housing of the oven with front ends, [7].

The station for ceiling welding (Figure 6) has the following key features:

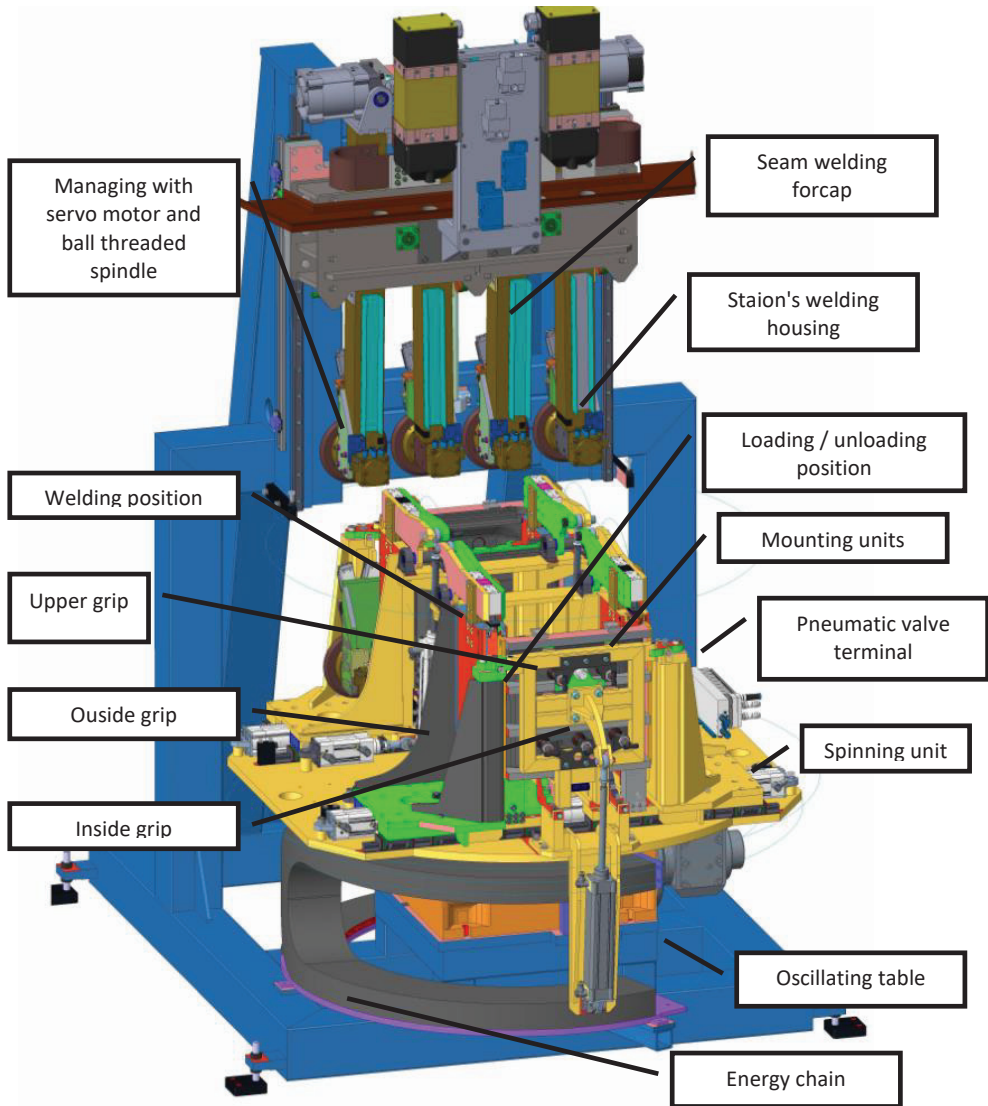


**Figure 6:** Final station for oven ceiling welding, [7]

Because of short deadlines, designing this kind of station is a process in which it is necessary to accept the decisions that affect the reliability, power consumption, welding quality, dimensions, appearance and price. All these criteria must be optimally coordinated for the success of a project. We can highlight two arguments among all the others.

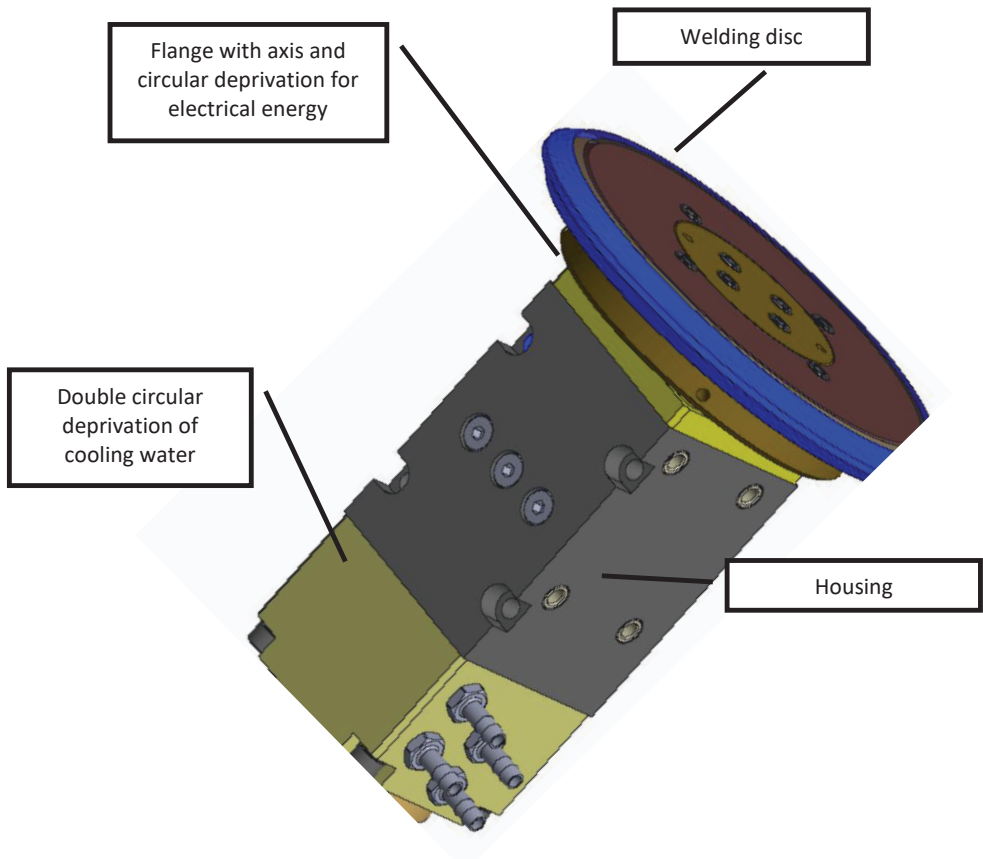


**Figure 7:** Seam welding unit, [7]

The transition of electrical energy from the frame to the rotary axis is executed with a special space that is sealed and contains a conducting material. Previously, mercury was used, but it is currently forbidden because of environmental standards. Because of welding and the enormous amount of conducting electrical energy, conduction heating occurs. Extraction of that heat is ensured with the supply of cooling water. Two units for seam welding are installed on the seam welding forceps, (Figure 7), [6-7].

Forceps for seam welding are vital at that station, among the correct mounting of the sheets. Actuating valves ensure the force needed for welding (Figure 8).

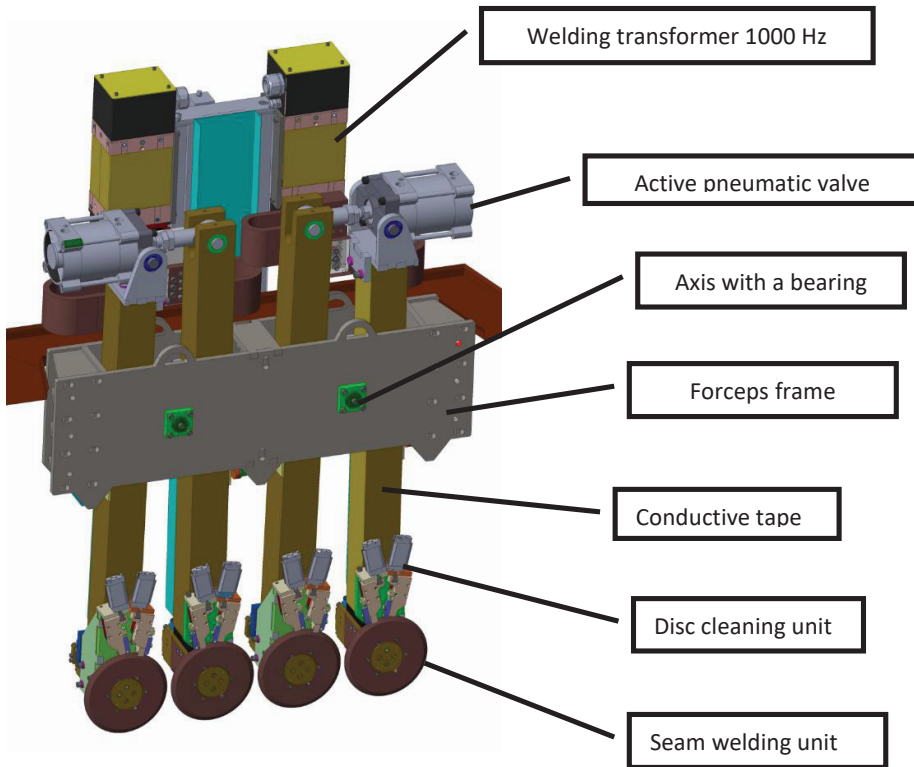


**Figure 8:** Seam welding forceps, [7]

Through tests that were made at different line and welding components, it was concluded that two seam welders were needed for each welded joint to ensure quality welding. The previous version of the station (2008) contained a seam on a straight electrode. This worked but no longer ensures sufficient quality for new demands; the sheet on the inner side was not adequately merged to the ceiling; therefore, an edge was visible. Implementing seam forceps improved the quality of the final product, [5-10].

The cooling is determined according to the type of weld, the number of welds per minute, the size of the current, and the cross-section of secondary conductors. Direct cooling of the tip of the electrode would be ideal, as shown in Figure 9. In that manner, a direct extraction of the heat is ensured. The life span is extended, and the welding lenses and joints are of higher quality, [7].



**Figure 9:** The position of weld joint that prevents U-circumference and ceiling deviation, [7]

When we are done with a weld joint, the welding disk performs a down move to a position 2 mm above the bottom edge of the oven (Figure 10). The disks must be moved as close to the edge of the oven as possible, so that the deviation of the U-circumference and the ceiling of the oven is prevented (Figure 11, Figure 12).



**Figure 10:** Bottom position of seam weld, [7]

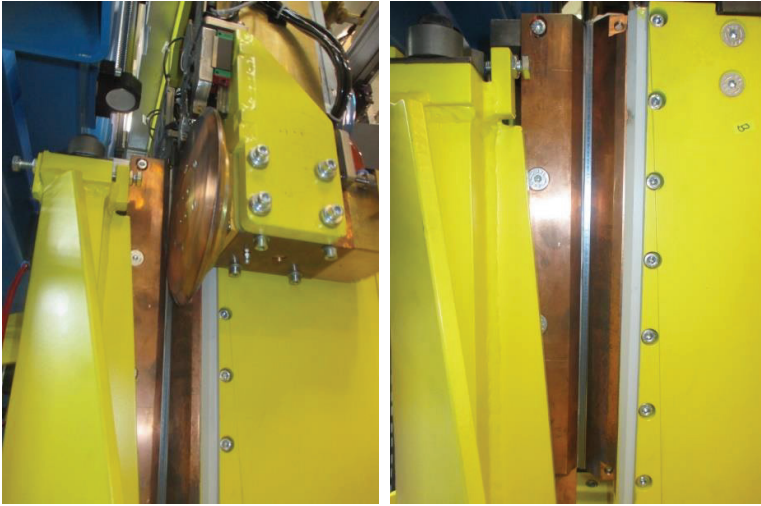


**Figure 11:** Upper position of seam weld, [7]



**Figure 12:** An example of welded U-circumference and front end, [7]

The BOS 6000 program is specially adapted to manage all BOSCH controllers. The program enables adapting the blocks and welding programs. In each block or program, we can set the required parameters, such as time of pre-pressing, pressing, welding, cooling, etc. Among the time parameters, the type of welding (point, seam) and the pressure of the seams to the welders can also be set.

## 4 CONCLUSIONS

The content of delta ferrite strongly affect the project life-span prediction, hot cracking, stress corrosion cracking and solidification cracking. The expected value of ferrite content in the weld material is from 2 to 5%.

The ferritoscope is the most useful tool for measuring delta ferrite because of its portability; the equipment is simple to operate and provides a direct non-destructive response for different types of stainless steels.

The calibration samples are correlated with ferritoscope magnetic response, and a specific calibration curve is configured in the equipment.

The current work made a careful analysis of the ferrite content results achieved by the ferritoscope and presents a proper selection of austenitic stainless steel for the production of ovens using the resistance seam welding process. The results of the study show that the amount of  $\delta$ -ferrite influences the quality assessment of austenitic stainless steel welds for the production of ovens by a resistance seam welding process.

The basic device of resistance seam welding for the production of stainless steel welds is manufactured. The device itself will have a huge role in the operation of the line; therefore, it was very precisely constructed and designed.

## References

- [1] **H. Bhadeshia:** *Steels: Microstructure and Properties* (Fourth Edition), New York, 2017
- [2] **M. Morinaga:** *A Quantum Approach to Alloy Design*, London, 2019
- [3] **V. Kain:** *Stress Corrosion Cracking*, New York, 2011
- [4] **S.G.Camerini, V.M. Silva:** *Ferrite content meter analysis for delta ferrite evaluation in superduplex stainless steel*, *Journal of Materials Research and Technology*, Volume 7, Issue 3, Pages 366-370, July–September 2018
- [5] **M. Brajar:** *Vpliv delta ferita na varivost jekel za energetiko : magistrsko delo*. Krško:
- [6] **Z. Praunseis:** *Energetski inženiring, Zapiski predavanj*, Fakulteta za energetiko, 2015
- [7] **S. Softić:** *Welding machine for cavity FS16 with resistance spot welding method*, *Master Thesis*, Faculty of energy technology, 2016
- [8] **B. Hudej:** *Koncipiranje in snovanje postaje za varjenje stroja pečice: diplomsko delo – Maribor*, Fakulteta za strojništvo, 2016
- [9] **Z. Praunseis:** *Točkovno uporovno varjenje nerjavnega bobna pralnega stroja, tehniško poročilo o raziskavi*, Fakulteta za strojništvo, 2003
- [10] **T. Sundararajan, Z. Praunseis:** *The effect of nitrogen-ion implantation on the corrosion resistance of titanium in comparison with oxygen- and argon-ion implantations*. *Mater. technol.*, 2004, vol. 38, no. 1/2



# IMPACTS OF ZERO-EMISSION POWERTRAINS BASED ON HYDROGEN TECHNOLOGIES IN PUBLIC TRANSPORT

## VPLIVI UPORABE NIZKO-EMISIJSKIH POGONSKIH SKLOPOV NA PODLAGI VODIKOVIH TEHNOLOGIJ V JAVNEM TRANSPORTU

Niko Natek<sup>31</sup>, Boštjan Krajnc<sup>1</sup>

**Keywords:** Hydrogen, Fuel Cell, Transport, Energy efficiency, Green-house gas emissions, EU, Energy transition, Environment, Public transport service, Internal combustion Engine, CO<sub>2</sub>

### **Abstract**

This article reviews the development potentials and environmental impact of introducing category M3 vehicles (for passenger transport/buses) with fuel cell electric powertrains to an urban and inter-urban public transport service (PTS) to be operated in the Savinjsko-Šaleška region. The main focus is the demonstration of the PTS modelling and preliminary environmental impact assessment of the operation compared to conventional (modern) diesel-powered internal combustion engines.

### **Povzetek**

Ta članek preučuje razvojne potenciale in vplive na okolje na primeru uvedbe vozil s pogonom na gorivne celice kategorije M3 (vozila za prevoz potnikov/avtobusi) za obratovanje v mestnem in medmestnem javnem prometu v Savinjsko-Šaleški regiji. Glavni poudarek je prikaz modeliranja storitve javnega prevoza in izvedba predhodne ocene učinka na okolje v primerjavi s klasičnimi (sodobnimi) dizelskimi motorji z notranjim zgorevanjem.

<sup>31</sup> Corresponding author: Niko Natek, Tel.: +386 3 896 1520, Fax: +386 3 896 1522, Mailing address: KSENA - Energy Agency of Savinjska, Šaleška and Koroška Region, Titov trg 1, 3320 Velenje, Slovenija; E-mail address: [niko.natek@kssena.velenje.eu](mailto:niko.natek@kssena.velenje.eu)

<sup>1</sup> KSENA - Energy Agency of Savinjska, Šaleška and Koroška Region, Titov trg 1, 3320 Velenje, Slovenija

## 1 INTRODUCTION

Sustainable mobility is recognized as one of the key areas of intervention within Europe's ambitious endeavour to address issues related to climate change and its high dependence on fossil fuel imports. Transport currently accounts for approximately one quarter of the EU's greenhouse gas emissions (GHG) and represents the lifeblood of the connected economies within the block. GHG emissions are, of course, only one part of the wider negative externalities (environmental and health costs) associated with transport, which are currently not taken into account to a sufficient degree.

Developing more efficient and less environmentally detrimental means of mobility while maintaining high transportation flows and excellent connectivity essential to a robust economy will be critical for achieving the targets of the European Green Deal, which pursues a 90% reduction of said emissions by 2050. The transnational policy of the EU is, among rail and inland waterways (with the core principle of multimodality), highly focused on facilitating wide market uptake of cleaner road vehicles and alternative fuels. One of its objectives is to achieve not less than 13 million zero and low-emission vehicles on European roads, that will be serviced by approximately one million public recharging and refuelling stations by as early as 2025. Whether or not this very ambitious objective is attainable and, in the end, beneficial to our society overall, will very much depend on administrating a pragmatic approach that will curb expenses and provide wider benefit to the EU economy and social cohesion. In this respect, the debate on which technologies would be most well suited to achieve these goals is ongoing and full of opposing opinions from different interest groups, while the only legitimate claim is that the advantages and inadequacies of individual technologies are highly dependent on specific use cases and cannot be generically declared to be superior or inferior for a broad area of applications.

This article will examine the performance of fuel-cell electric (FCEV) powertrain technology with hydrogen as the main energy carrier compared to conventional (high-efficiency, diesel-powered) internal combustion engines (ICE) on the example of a planned zero-emission urban and inter-urban public transport service (PTS) in the Savinjsko-Šaleška region of Slovenia. The article is derived from the main results achieved by the efforts of the City municipality of Velenje to establish a zero-emission PTS that would help drive the energy transition and decarbonization of the region.

## 2 FRAMEWORK AND POLICY BACKGROUND

Slovenia has formally declared ambitious targets in the areas of decarbonization, low-carbon energy, and transport. The core legislative framework for the energy sector, in general, is outlined in the new Energy Act, [1], from 2014, which in the context of supporting the energy transition defines some essential provisions, for example, in Chapter II on increasing energy efficiency (EE) and the use of renewable energy sources (RES). Articles 314 to 316 define how EE and RES shall be supported and also the types of financial incentives provided by the state for this purpose. Article 317 defines the "contribution for energy efficiency" (an important funding source for the national environmental fund – Eko sklad) paid by final users for energy from district heating, electricity, solid, fluid and gas energy carriers. Grants (non-refundable) and soft-loans provided through the Eko sklad are an essential driver of supporting initial investment into sustainable mobility, which is provided for various vehicle categories (motorcycles, passenger cars, light-duty

vehicles, buses and coaches, heavy-duty transport) with electric or hybrid powertrains. Eko sklad also manages certain investment support schemes provided by the Fund for Climate Change (Sklad za podnebne razmere) financed in accordance to Article 129. of the Environmental Protection Act (ZVO), which stipulates that the provision from the sale of emission coupons obtained through auction are used for providing financial support to climate mitigation measures. The major contributor to the fund is the Šoštanj thermopower plant (TEŠ).

Specific actions and sector-related targets are outlined in targeted action and operational plans, which are due for revisions for the post-2020 period. These include the National Renewable Energy Action Plan (NREAP) (Akcijski načrt za obnovljive vire energije za obdobje 2010-2020 - AN OVE), [2], the Operational Programme for limiting greenhouse gas emissions until 2030 (Operativni program ukrepov zmanjšanja emisij toplogrednih plinov do leta 2030 (OP TGP)), [3], and the National Energy Efficiency Action Plan (NEEAP) (Akcijski načrt za energetska učinkovitost (AN URE 2020)), [4].

Core national targets/milestones up to the year 2020 that have been defined within these operational and action plans include:

- **Milestone 1** – 25% share of RES in gross final energy supply (AN OVE, 2017)
- **Milestone 2** – Increasing energy efficiency by 20% up to 2020, defined as a threshold of total primary use not exceeding 7.125 Mtoe ( $\approx 82.86$  TWh) or a maximum 2% annual increase cap (AN URE)
- **Milestone 3** – Meeting obligations on the reduction of GHG emissions, by capping maximum annual increases to no more than 4% from the base year 2005, i.e., total emissions will not exceed 12.117 kt of CO<sub>2</sub> equivalent in 2020 (OP TGP).

Milestone 1, which is specified for RES shares in specific sectors in accordance with the Renewable Energy Directive 2009/28/ES that targets a 25% share of RES in gross final energy supply and a 10% share of renewable energy in transport, likely will not be met by the end of 2020 even though the Ministry of Infrastructure has already outlined additional measures to be implemented to mitigate the shortfall. In the context of milestone 2, it was already achieved several years ago, mostly due to substantially reduced economic activity (the aftermath of the financial crisis of 2008) and has not surpassed the threshold (in 2017 it reached roughly 77.23 TWh). Concerning Milestone 3, the operational programme is limited to non-ETS sectors; thus, no direct measures for entities included in the scheme as well as for reducing indirect emission resulting in energy use are outlined. The emission cap is provided for non-ETS sectors, which account for about 59% of total CO<sub>2</sub> equivalent emission that reached 19,509 kt CO<sub>2</sub> in 2014 when the operational plan was published.

The main driver for decarbonization of the energy sector is, therefore, the implementation of the ETS, in which carbon allowances have increased more than 400% from May 2016 (from a low of €5,72 to over €25 per tonne of CO<sub>2</sub>) to 2019 respectively. The implementation of the 4th stage of the ETS from 2021 onwards, which will increase the rate of annual reductions of available allowance to 2.2% will further exacerbate the already poor economics of energy production at TEŠ.

Strong expectations were placed on the development of the Energy Concept of Slovenia (Energetski Koncept Slovenije (EKS)) or the Resolution on the energy concept (ReEKS), [5], planned to be adopted by the parliament in the first half of 2020. The EKS provides two core orientation milestones of reducing energy-related GHG emission by at least 40% by 2030 and at

least 80% by 2050, compared to the baseline year of 1990. At present, the most up-to-date strategic development addressing the decarbonization in the comprehensive context of the energy transition is the National Energy and Climate Plan (Nacionalni energetska in podnebni načrt – NEPN), [6], that is based on EU resolutions on establishing a reliable and transparent system for managing the energy union (2014), resolutions n. 14459/15 on the mandatory development of national plans for member states by the end of 2019 (205) and the Decree 2018/1999 instituted at the end of December 2018 on the management of the energy union and climate change mitigation measures. Core objectives and milestones from the existing legislative framework are reinstated and collected within NEPN, which expands the development focus to 2030 and beyond to 2050. It comprehensively addresses several areas pertinent to carrying out the energy transition, from environmental aspects to socio-economic (research and innovation) implications. While the target on RES in gross final energy supply is increased to at least 27% until 2030 whereby the cap for final energy use is imposed at 54.9 TWh, transport plays an important role in the declared strategy. By 2030, at least 21% of the energy used in transport will be renewable (11% of bio-/alternative fuels) and transport will decrease its GHG emission by 12% overall. NEPN specifically indicates that Slovenia will support the development of infrastructure for alternative fuels in transport (including liquefied natural gas, compressed natural gas and hydrogen) and further electrification of transport also indicated in the Alternative Fuels Strategy (Strategija na področju razvoja trga za vzpostavitev ustrezne infrastrukture v zvezi z alternativnimi gorivi v prometnem sektorju v Republiki Sloveniji) adopted in 2017. The strategy also stipulates that special attention will be provided to supporting energy-efficient and clean public transport. Furthermore, NEPN specifies the support to pilot projects for producing synthetic methane and hydrogen with an indicative objective to achieve a share of synthetic methane and hydrogen in the transmission and distribution gas grid at 10% by 2030.

In 2017, Slovenia's energy dependency rate was 48%. Generation of energy from non-renewable RES (PV, wind energy) is problematic for the stability of the electricity system, and a high proportion of such sources will require significant investments in upgrading existing infrastructure, in particular energy transmission, distribution and storage/regulation systems. Current trends in the field of electro-mobility (along with the trend of electrification of heating systems) indicate, among other things, a significant increase in the share of battery electric vehicles (BEV) in transport (and an overall increase in electricity use), which does not offer an appropriate long-term sustainable solution to Slovenia's energy situation and development targets. It creates a number of additional problems, the primary question of which is, among many others, that of providing additional electricity generation capacities (substantial public resistance to investment is already being made, even in RES, e.g., in the projects of Volovja Reber, HPP on the Mura River) and more importantly, significant investments in transmission/distribution networks, energy storage, etc. that could lead to high energy prices for households and make the economy uncompetitive. Energy investments should be designed in a comprehensive manner that will, to the greatest extent, allow the Slovenian economy to be involved in the development, production and maintenance of the installed infrastructure in the wider context of available natural resources (human resources, energy, critical raw materials (CRMs)). With many hydrogen applications still being a relatively underdeveloped market, domestic businesses have tremendous opportunities to develop and promote their high value-added products and services in European and global markets.

### 3 HYDROGEN TECHNOLOGIES IN THE SAŠA REGION

The ambition to implement hydrogen technologies as an important part of sustainable development efforts of the region is based on over 10 years of activities related to planning, technical analysis, stakeholder engagement, and consultation, as well as research and pilot testing. The requirement for hydrogen as a coolant for generators of the Šoštanj thermopower plant (TEŠ), which was originally fired by locally mined lignite, was first signified after the concluded construction of power unit 3 in 1960. With the following construction of units 4 and 5, these requirements increased to the point that the management of TEŠ decided to establish on-site hydrogen production. Due to high awareness that energy production from lignite is limited in time and accessible reserves as well as the outstanding commitment of the company and local communities to reduce negative environmental impacts caused by energy production, TEŠ joined the Centre of Excellence on Low-Carbon Technologies (CONOT), where they began a research project titled “Hydrogen technologies in advanced energy supply” alongside 22 partner organizations including renowned research institutions and high-profile companies. Within the scope of the project, CONOT established an experimental hydrogen production unit (alkaline electrolysis), which is still in operation today and has a maximum capacity of 15 Nm<sup>3</sup>/h.

The hydrogen is produced by alkaline water electrolysis that utilizes potassium hydroxide (KOH) for enhancing the conductivity of the electrolyte solutions. The on-site hydrogen generator (type HYSTAT-A 1000/15/25 from Hydrogenics with a single cell stack) is powered through a transformer (3 × 400 V~/250 V=) with 250 V and 376 A direct current. Obtained gasses (H<sub>2</sub>, O<sub>2</sub>) are stored in pressurized containment vessels. The unit can deliver gaseous hydrogen at 2500 kPa (25 bar) without the use of an additional external compressor, which helps to reduce the overall energy consumption (highest energy-consuming stage of the compressor from 1 to 10 bars is excluded) of the unit, as well as to avoid electrolyte losses that are typical for atmospheric electrolyzers. The low energy consumption of the cell stack is 4.2 kWh/Nm<sup>3</sup> and 4.9 kWh/Nm<sup>3</sup> on the level of the unit is the result of a highly conductive membrane and catalysed electrodes constructed in a so-called “zero-gap” configuration (reduced drops in voltage). The unit offers highly flexible production in the range of 25% to 100% output by adjusting the current density on the cell stack. HYSTAT-A also offers flexibility in terms of compatibility with optional equipment (closed-loop cooling systems, reversed osmoses systems, deoxo-driers, compressors, etc.) that can provide a tailor-to-fit to specific user requirements. Additional features include integrated safety, fully automated operation, compact and flexible modular design (capacity determined by the number of cells incorporated in the unit), easy installation and the ability for direct coupling with a DC renewable energy source (input of fluctuating currents). The production unit is now primarily used to supply the technical tasks of power plant maintenance with oxygen while hydrogen is being used mainly for the cooling of electrical generators. The demand for oxygen exceeds the demand for hydrogen; therefore, a substantial amount is vented to local surroundings. On average, TEŠ generates about one third of electrical energy in Slovenia but can operate to supply more than half of the national demand. With an installed power of 1304 MW, it produces from 3500 to 3800 GWh of electrical energy on an annual basis but also supplies heat to the Šaleška Valley by a district heating system in the amount of 300 to 350 GWh. For annual operation, it requires from 3.5 to 3.8 million tons of lignite supplied by the local mine, Premogovnik Velenje, [7].

The vision of CONOT at that time also included the establishment of a hydrogen refuelling station and mobile assets that would operate in the Savinjsko-Šaleška region, which unfortunately did

not come to fruition due to external factors related to poor economic status and subsequent lack of political will. CONOT was, however, successful in establishing one of the two originally planned hydrogen refuelling stations in Lesce (first HRS in Slovenia) in 2013 but did not anticipate the slow development of commercial hydrogen vehicles; therefore, the actual operation of the station was negligible. The failure to plan for actual hydrogen demand was a significant flaw of the project approach, which has almost entirely halted additional capacity development in the field to this day. Nevertheless, the increasing political and economic (carbon allowances) pressure on coal-fired energy production mandates that the powerplant, as well as the local and national authorities, actively seek a feasible development strategy that would allow for the gradual substitution of energy production from lignite (on average provides over one third of electrical energy production on the national level) taking into account the significance of a wider range of technical (energy production and storage), environmental (reduction of GHG and pollutants) and socio-economic (employment, supporting knowledge-intensive industries and innovation, etc.) factors.

Under the leadership of the Municipality of Velenje, the deployment of hydrogen technologies was approached again in 2017 and confirmed with the adherence to the Fuel Cells and Hydrogen Joint Undertaking (FCH JU) Regions and Cities initiative to address the targets related to green mobility and emissions reduction of the municipality outlined in the local strategic documents.

## 4 MODEL PUBLIC TRANSPORT SERVICE

Since 2008, the municipality of Velenje has operated a public transport service under the name “Lokalc” that was developed with a purpose to increase the efficiency of urban transport within the area by offering citizens, employees and visitors an alternative to their private passenger vehicles. To support wide uptake of the service, it was designed and remained free of charge providing simple access for its entire time it operated. Today the PTS operates 5 lines with 43 stations, which are serviced by diesel-powered minibuses with EURO5 and EURO6 emission ratings. On average it accommodates approximately 35,000 passenger trips per month (2018) and has proven to be highly successful in reducing the number of vehicles used for transport along with all their negative externalities.

The model for the zero-emission PTS builds on the experience with Lokalc followed up by a comprehensive stakeholder dialogue with the local community as well as detailed planning process with internal experts, public transport operators and private companies to determine optimal routes for the renewed service. The zero-emission PTS is structured by seven routes that encompass over 500,000 km of travelled distance annually and target service over 410,000 passengers annually. The routes connect the key interest areas of the Municipality of Velenje and the Municipality of Šoštanj, as indicated in Figure 1.

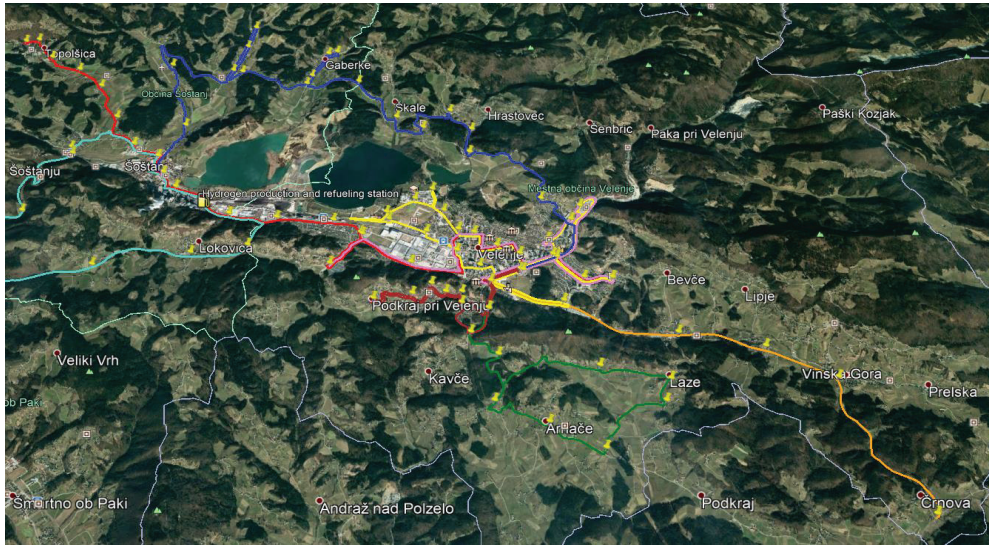


**Figure 1:** Modelled routes for the zero-emission PTS

#### 4.1 Route analysis

The analysed routes are assumed to be operated by 6 (six) fuel-cell electric M3 category vehicles, model “Businova hydrogen Midibus”, which is a 10.5 metre-long urban bus powered by a 32 kW PEM Michelin fuel-cell and a 132 kWh buffer and range extender battery. The vehicle is capable of storing 30kg of hydrogen at 350 bars, allowing for vehicle autonomy of over 350 km. The routes and respective distribution of vehicles to the public transport service is structured to require only one refuelling cycle per day. The modelling took into account different consumption scenarios in terms of the average number of people using the service, driving mode, air conditioning and thermal management requirements (six basic scenarios) for each route according to the predeveloped travel itineraries. The modelling scenarios were determined for two passenger loads (at 25 and 45 passengers) and three thermal management regimes (power consumption levels between heating and AC switched off and full power: 0, 3, and 5 kW of nominal power consumption respectively, [9]). The modelling approach for the yellow line (Rumena progá) is represented in Figure 2 and Table 1 below:

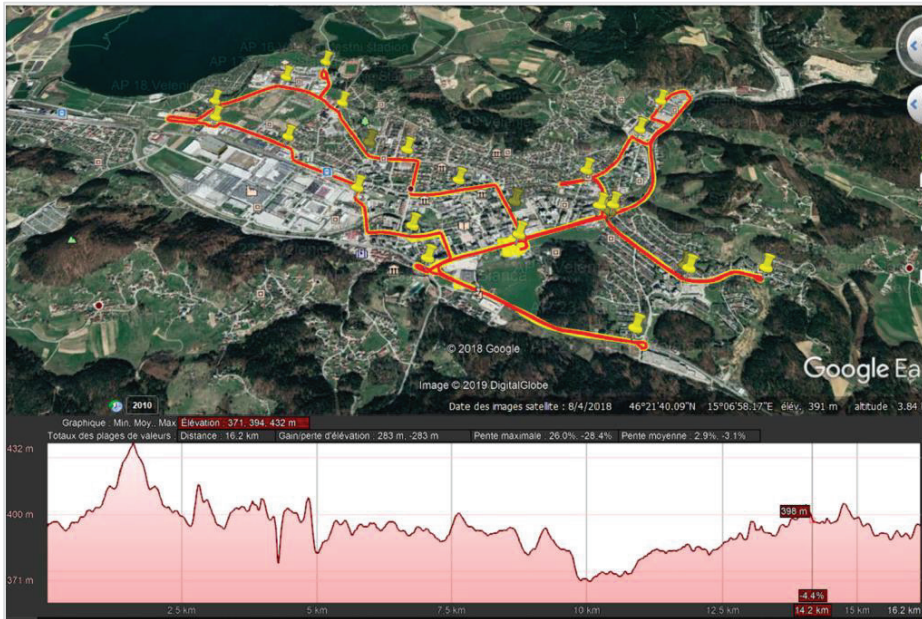


**Figure 2:** Yellow route overview (stops, route, incline) with Keyhole Markup Language

The modelling analysis of the route is carried out on the assumption that the useful mass of hydrogen stored in the tanks that can be utilized by the fuel cell equals 29.1 kg. The case presented in Table 1 builds on the premise that all of the energy required to operate the vehicles is supplied from the hydrogen only whereby the energy from the battery is only used as a buffer (to provide continuous power supply to the electric engine) which represent the nominal mode of vehicle operation. It is also possible to apply the maximum energy stored in the energy to increase vehicle autonomy, which can increase easily above 400 km. In terms of nominal vehicle operation, it was found that an average consumption between 7.5 and 8 kg of hydrogen per 100 km can be easily achievable in eco-driving mode (utilizing regenerative braking) which would bring the autonomy range to a minimum 339 km in the highest load configuration (not realistic everyday operation but rather a highly conservative estimate of vehicle capability). The results are presented in Table 1 below:

P. *	Thermal management (kW)	Traction energy (kW/km) *	Auxiliaries energy (kW/km) **	Regeneration (kW/km) ***	Total energy (kWh/km)	Daily H2 consumption (kg)	Battery SOC final (%)	Autonomy range (km)	Hydrogen consumption (kg/100km)
25	0	1.012	0.173	-0.243	<b>0.942</b>	29.1	90%	<b>448</b>	<b>6.50</b>
	3	1.012	0.302	-0.243	<b>1.071</b>	29.1	90%	<b>392</b>	<b>7.43</b>
	5	1.012	0.389	-0.243	<b>1.158</b>	29.1	90%	<b>363</b>	<b>8.02</b>
45	0	1.096	0.173	-0.244	<b>1.024</b>	29.1	90%	<b>410</b>	<b>7.09</b>
	3	1.096	0.302	-0.244	<b>1.154</b>	29.1	90%	<b>364</b>	<b>8.00</b>
	5	1.096	0.389	-0.244	<b>1.240</b>	29.1	90%	<b>339</b>	<b>8.59</b>

**Table 1:** Modelling results for the yellow route according to baseline scenarios

Table 1 demonstrates the modelling results for operating the yellow route under different passenger loads and thermal management requirements. The modelling is based on the assumption that no thermal management is required when the external temperature is between 15 and 22° C, moderate thermal management is required to power the AC unit when outside temperatures are in the range from 23 to 28° C or below -5° C to power the additional resistor heaters, and maximum thermal management is required for temperatures above 28 and below -5°C. The average assumed weight for the individual passenger is 70 kg, excluding the driver. The results of the modelling for all seven routes are presented in Table 2.

Route/ Parameter	Blue	Orange	Red	Brown	Yellow	Turquoise	Violet	Green	Total
Travelled distance (km/day)	390.78	63.76	639.58	31.21	696.34	65.57	45.26	49.20	<b>1981.69</b>
Travelled distance (km/year)	101948.64	16634.03	166855.78	8141.70	181665.18	17104.93	2353.52	12835.54	<b>507539.32</b>
Operational hours (h/year)	1948.88	466.72	7769.94	313.06	8493.51	521.77	97.07	417.42	<b>20028.36</b>
Fuel economy (kg H <sub>2</sub> /100km)	8.01	6.23	6.94	7.98	6.93	6.20	6.75	8.22	<b>7.16</b>
Hydrogen consumption (kg/day)	31.30	3.97	44.39	2.49	48.26	4.07	3.06	4.04	<b>141.57</b>
Hydrogen consumption (kg/year)	8166.09	1036.30	16542.56	649.71	14638.83	1060.51	158.86	1055.08	<b>43307.94</b>
Average speed (km/h)	52	36	21	26	21	33	24	31	<b>30.58</b>
No. of refuelling (no./IND)	1.043	0.132	1.480	0.083	1.609	0.136	0.102	0.135	<b>4.72</b>
No. of stops (no.)	24	11	24	8	21	13	16	8	/

**Table 2: Main results of route modelling**

## 5 ENVIRONMENTAL IMPACTS

The baseline assumption of the preliminary environmental impact assessment presented in this article is that the hydrogen used to operate the PTS is sourced from highly efficient production methods that require little to no additional energy input (specifically in the case of the analysed project; this could be achieved within the requirements/capacity of grid balancing, i.e., powering down the operation of the thermopower plant or by means of waste gasification). This remains feasible while the amount of required hydrogen is at a relatively low scale, compared to the overall production capacity of either the thermal power plant or in terms of gasification, when the input raw material includes various types of carbonaceous waste (biomass, municipal waste, wastewater treatment sludge, etc.). In this respect, the approach of quantification is similar as to consider these available sources as energy that would otherwise need to be curtailed or simply not applied, meaning that the life-cycle impact assessment from primary energy (lignite) to

hydrogen can be avoided. In reality, a certain amount of energy would need to be considered to account for the impact of required equipment and infrastructure; therefore, baseline assumptions used in the calculations are highly conservative in order to compensate for this effect, while primary impacts are focused on triggering energy savings and renewable energy production (in the form of alternative fuel). The secondary impacts are mostly attributed to other direct benefits derived from the deployment of the zero-emission PTS, including GHG and pollutant emissions (NO<sub>x</sub>, HC, CO and PMs) reduction directly due to the PTS operation and indirectly as a result of reduced use of personal vehicles in urban trips and improved access to public transport.

## 5.1 Energy savings triggered

The energy savings triggered by the project are determined based on preliminary design and analysis of the new zero-emission PTS, compared to the current energy use of the ongoing service Lokalc which deploys standard ICE vehicles with EURO5 and EURO6 diesel engines. The current operation of the Lokalc PTS has a scope of 320,000 kilometres of annual travelled distance to operate the existing routes. As mentioned before, the preliminary design of the renewed PTS indicates that to meet the needs of the various local and regional beneficiaries, the new routes should encompass a total distance of 517,000 km of annual travel.

In the technical report of the Lokalc operation, despite using much smaller and less accommodating vehicles, an average fuel economy of 25l of diesel per 100 km was recorded in 2017 and 2018. A volume of 1l of diesel fuel equals about 10kWh of energy, meaning that the total energy consumption based on the use of propellant fuel alone was about 800 MWh in 2017 to service the existing line, while the travelled distance of the new PTS would indicate a value of 1292.5 MWh of direct primary energy savings of the project which would decrease the use of diesel fuel 129,250 l of unused diesel fuel in relation the required travelled distance of the new zero-emission PTS.

The FCEVs comparatively use much less energy per travelled distance, due to the higher efficiency of the FCE drivetrain and regeneration braking (estimated at 1.5 kWh/km for fuel vehicle occupancy compared to the 2.5 kWh/km on average of the ICE vehicles currently in operation) so even a pessimistic scenario in which there is little available excess energy on peaks (which is not the case), the comparable operation would still entail an energy saving of 517 MWh less than the existing baseline. In addition, the preliminary design of the routes is planned to accommodate improved access to public transport with new stops, new routes, higher frequency on rush hours and overall optimized operation, meant to increase the individual trips with the PTS by at least 7% from 2017 when it was 421,198, which would entail an additional 30,000 additional trips with the PTS per annum. Based on the experience of the deployment of the existing Lokalc PTS, surveys with users and technical analysis indicated that at least one third of travellers opted out of using their own means of transportation when the service was made available. In the case of the renewed zero-emission PTS, this would encompass at least 10,000 individual trips with public transport instead of their car on a yearly basis. Considering an average 8,7 l/100 km fuel economy for urban driving and that each trip was calculated to be 6km, this signifies 60,000 km of mitigated passenger car travel distance. A 45% to 55% share of gasoline versus diesel-powered vehicles outlines a reduction of 2871 l and 2349 l of spent diesel and gasoline fuel respectively, amounting to a reduction of a total of 49.851 MWh (28,710 kWh of energy in diesel and 21,141 kWh in gasoline) of additional energy savings even by these very conservative assumptions. A total primary energy savings of at least 1.424 GWh would be achieved.

## 5.2 Renewable energy production triggered

The preliminary operation of the renewed PTS consists of 517,000 km of annual travel distance. Based on baseline route modelling, it would require about 140 kg of hydrogen dispensed at 350 bar or about 44 tons of annual production to service the required distance. In line with the assumed hydrogen production scenario, whereby only excess electrical energy within the HSE groups of producers is used in the electrolyser, the system will produce at least 1318.38 MWh of green hydrogen from energy that would be otherwise be curtailed/unused.

## 5.3 Reduction of GHG emissions by the operation of the PTS

Reduction of greenhouse gas emissions expressed as CO<sub>2</sub> equivalent is determined based on the existing LokalC PTS compared to the planned zero-emission PTS. Considering the 517,000 km of travel distance yearly, if it were to be operated by EURO5 end EURO6 as is the case today, the ICE vehicles would require a total of 129,250 l of diesel fuel. 1 litre of diesel weighs 835 g (gram). Diesel consists of 86.2% carbon, or 720 g of carbon per litre diesel. To combust this carbon to CO<sub>2</sub>, 1920 g of oxygen is needed, hence 2640 g of CO<sub>2</sub> is produced for every litre of burned diesel. Taking into account the current distribution of EURO5 and EURO6 vehicles in operation (approximately a 1:2 ratio), the total GHG emissions from fuel combustion amount to 341.22 t per annum.

## 5.4 Reduction of GHG emission by increased use of PTS (reduced use of personal vehicles)

Similarly, as presented for the previous example of the direct PTS GHG reduction and considering the calculations applied to determine primary impacts with relation to impacts of increased use of public transport (lowering inefficient transport with personal ICE vehicles), this will further decrease emissions by a minimum of 13.78 tonnes of CO<sub>2</sub> equivalent per annum.

## 5.5 Reduction of pollutant emissions by the operation of the PTS

The zero-emission PTS will also substantially reduce pollutant emissions relative to those ICE vehicles would emit during their operation (baseline). Considering the declared ratio of EURO5 and EURO6 operation (1:2), the former would operate cca. 172,330 and the latter 344,670 kilometres yearly, which indicates an average annual operation time of 22,188 hours (at 23.3 km/h average speed and 20 s delays at preliminary bus stops). EURO standards for heavy-duty diesel engines (steady-state testing for the conservative estimate) are declared in g/kWh (pollutant emission in gram as for a unit of produced energy). The emission ratings applicable to the EU declared with the World Harmonized Stationary Cycle (WHSC) are presented in Table 3 for the steady-state testing (notable difference between CO and PM emission compared to transient testing, [8]).

Stage	Date	Test	CO	HC	NOx	PM	PN	Smoke
			g/kWh				1/kWh	1/m
Euro III	1999.10 EEV only	ESC & ELR	1.5	0.25	2	0.02		0.15
	2000.10		2.1	0.66	5	0.1		0.8
Euro IV	2005.10		1.5	0.46	3.5	0.02		0.5
Euro V	2008.10		1.5	0.46	2	0.02		0.5
Euro VI	2013.01	WHSC	1.5	0.13	0.4	0.01	8.0×10 <sup>11</sup>	

<sup>a</sup> PM = 0.13 g/kWh for engines < 0.75 dm<sup>3</sup> swept volume per cylinder and a rated power speed > 3000 min<sup>-1</sup>

**Table 3:** Heavy-duty EU emission standards at steady-state testing (Source: Dieselnets.com)

The existing vehicles are rated at 132 kW power output of the ICE, which determines the following parameters in accordance with an operational time of 7396.28 and 14792.56 for hours per annum EURO5 and EURO6:

Vehicle/pollutant	CO	HC	NO <sub>x</sub>	PM
Emissions of EURO V	1464.46	449.10	1952.62	19.53
Emissions of EURO VI	2928.93	253.84	781.05	19.53
Total	4393.39	702.94	2733.67	39.05

**Table 4:** Pollutant emission reductions of FCEV compared to ICEs.

## 5.6 Reduction of pollutant emissions by increased use of the PTS

Emission ratings for light-vehicles are provided per travelled distance (mass in g per travelled km). The impact estimation implies a conservative scenario where all personal vehicles removed from their operation are EURO6.

Overview of emission reductions:

Indicator	Quantification		Unit
Reduction of GHG emissions by the operation of the PTS	Per annum	10 years	
	≈ 341.22	≈ 3400	t CO <sub>2</sub> eqv
Reduction of GHG emission by increased use of PTS	≈ 7.58 (diesel vehicles) ≈ 6.20 (gasoline vehicles)	≈ 137,8	t CO <sub>2</sub> eqv
Reduction of pollutant emissions by the operation of the PTS	≈ 4393.39 ≈ 702.94 ≈ 2733.67 ≈ 39.05	≈ 44000 ≈ 7000 ≈ 27300 ≈ 390	(kg/year) CO (kg/year) HC (kg/year) NO <sub>x</sub> (kg/year) PM
Reduction of pollutant emissions by increased use of the PTS	≈ 43.5 ≈ 2.97 ≈ 4.26 ≈ 0.36	≈ 435 ≈ 29,7 ≈ 42,6 ≈ 3,6	(kg/year) CO (kg/year) HC (kg/year) NO <sub>x</sub> (kg/year) PM

**Table 5:** Pollutant emission reductions by reduction of personal vehicles in transport

## 6 CONCLUSION

The benefits of introducing hydrogen technologies as demonstrated on the specific use case of applying FCEVs in public transport would be able to produce valuable environmental benefits and an effective step towards achieving several formal objectives related to sustainable development as formally adhered to by the Republic of Slovenia. However, positive wider benefits of such development far exceed the mere environmental benefits compared to conventional ICEs, but addresses cross-sectoral challenges based on the following core guidelines on which the energy transition would be programmatically built upon:

- highest possible use of local (domestically available) energy sources
- maximum integration of renewable energy sources in the national energy mix
- reduction of energy dependence (foreign energy imports)
- lowest achievable environmental impact of energy production and use
- maintain the stability of the transmission grid and distribution system
- implement investments with the potential to support research, innovation and development and the development of valuable skills for employees required by enterprises in knowledge-intensive industries
- support of international promotion
- contribute to the development of sustainable (green) tourism in the region.

Such deployment projects could be structured to support further technology and market development of both the Slovenian and the EU's automotive industry. The potential to establish synergies with other innovative technology applications (such as gasification of waste) could represent a major step towards achieving an economically sustainable circular economy on the transnational level. The potential to support the gradual transition of coal-intensive regions with this approach is immense, and the overall concept is relevant to and directly applicable in several countries/regions within and outside the EU, which are pressured to actualize the energy transition within a relatively short time basis but have no clear, comprehensive plan on how this could be achieved, especially in consideration of the resulting negative impacts on employment

## References

- [1] Energy act EZ-1, Official Gazette of the Republic of Slovenia, 2014  
Available: <http://www.pisrs.si/Pis.web/pregledPredpisa?id=ZAKO6665> (accessed 5.5.2020)
- [2] **Ministry of Infrastructure of the Republic of Slovenia**, National Renewable Energy Action Plan (AN OVE), 2017  
Available: [https://www.energetika-portal.si/fileadmin/dokumenti/publikacije/an\\_ove/posodobitev\\_2017/an\\_ove\\_2010-2020\\_posod-2017.pdf](https://www.energetika-portal.si/fileadmin/dokumenti/publikacije/an_ove/posodobitev_2017/an_ove_2010-2020_posod-2017.pdf) (accessed 5.5.2020)
- [3] **Government of the Republic of Slovenia**, Operational programme for limiting greenhouse gas emissions until 2020, 2014  
Available: [https://www.energetika-portal.si/fileadmin/dokumenti/publikacije/op\\_tgp/op\\_tgp\\_2020.pdf](https://www.energetika-portal.si/fileadmin/dokumenti/publikacije/op_tgp/op_tgp_2020.pdf) (accessed 5.5.2020)
- [4] **Jožef Stefan Institute et al.**, National Energy Efficiency Action Plan - AN URE, 2017  
Available: [https://www.energetika-portal.si/fileadmin/dokumenti/publikacije/an\\_ure/an\\_ure\\_2017-2020-jo.pdf](https://www.energetika-portal.si/fileadmin/dokumenti/publikacije/an_ure/an_ure_2017-2020-jo.pdf) (accessed 5.5.2020)

- 
- [5] **Ministry of Infrastructure of the Republic of Slovenia et al.**, Resolution on the Energy concept of Slovenia, 2018  
Available: [https://www.energetika-portal.si/fileadmin/dokumenti/publikacije/eks/resolucija\\_eks/re-eks\\_jo\\_avg\\_2018.pdf](https://www.energetika-portal.si/fileadmin/dokumenti/publikacije/eks/resolucija_eks/re-eks_jo_avg_2018.pdf) (accessed 5.5.2020)
- [6] **Jožef Stefan Institute et al.**, National Energy and Climate Plan, 2018  
Available: [https://www.energetika-portal.si/fileadmin/dokumenti/publikacije/nepn/dokumenti/nepn\\_5.0\\_final\\_feb-2020.pdf](https://www.energetika-portal.si/fileadmin/dokumenti/publikacije/nepn/dokumenti/nepn_5.0_final_feb-2020.pdf) (accessed 5.5.2020)
- [7] **B. Krajnc et al.**, Investment programme: Hydrogen technologies in zero-emission transport. City municipality of Velenje, 2019
- [8] **European Commission**, Heavy duty EU emission standards at steady-state testing (website publication based on Regulation (EC) No 595/2009 of the European Parliament and of the Council and amendments  
Available: <https://dieselnet.com/standards/eu/hd.php> (accessed 5.5.2020)
- [9] **Société Albigeoise de Fabrication et de Réparation Automobile**, Businova H2 preliminary technical information - Supply of Fuel Cell buses: Businova H2 Midibus L (10,5 meters), 2019

# A SIMPLIFIED HYBRID METHODOLOGY FOR DESIGNING CORELESS AXIAL FLUX MACHINES

## POENOSTAVLJENA METODA ZA NAČRTOVANJE SINHRONSKIH STROJEV S TRAJNIMI MAGNETI IN AKSIALNIM MAGNETNIM PRETOKOM BREZ FEROMAGNETNEGA JEDRA STATORJA

Franjo Pranjić<sup>1,✉</sup>, Peter Vrtič<sup>1</sup>

**Keywords:** Axial flux permanent magnet generator (AFPMG), approximation method, magnetic flux, magnetic flux density

### **Abstract**

Axial flux permanent magnet generators (AFPMG) are used in many high torque applications, including wind generators. There are many design methodologies for AFPMG that are connected to simple design equations used for preliminary design. Analytical methods offer a fast preview of torque production of the designed machine with a certain degree of accuracy. The finite element method (FEM) is a more accurate numerical method than other methods and requires a great deal of time for simulations in the design procedure. This article presents a method for the design and analysis of an axial flux permanent magnet generator by using approximation polynomials.

<sup>✉</sup> Corresponding author: Franjo Pranjić, Tel.: +386 3 777402, Mailing address: Koroška cesta 42a, E-mail address: franjo.pranjic@um.si

<sup>1</sup> University of Maribor, Faculty of Energy Technology, Hočevarjev trg 1, 8270 Krško

## Povzetek

Sinhronskih generatorji s trajnimi magneti in aksialnim magnetnim pretokom (SGTMAMP) se uporabljajo v mnogih aplikacijah kjer so zahtevane visoke vrednosti navora, kot npr. za generatorje vetrnih elektrarn. Obstaja veliko metodologij za načrtovanje teh strojev, ki so povezane z analitičnimi enačbami za preliminarno načrtovanje tega tipa strojev.

Analitične metode ponujajo hiter predogled proizvodnje navora načrtovanega stroja z določeno stopnjo natančnosti. Numerične metode, in sicer metoda končnih elementov (MKE), so natančnejše od drugih metod in zahtevajo veliko časa za simulacije v postopku načrtovanja. V tem članku je predstavljena metoda za načrtovanje in analizo SGTAMP z uporabo aproksimacijskega polinoma.

## 1 INTRODUCTION

Axial flux permanent magnet generators (AFPMG) have simple constructions, are compact, have a high degree of reliability and high-power density, [1-7]. They are also called “disk-type” machines and have various topologies, depending on the application: single-sided (one stator and one rotor) shown in Fig.1; double-sided (single stator-double rotor or single rotor-double stator [6]) shown in Fig.2-Fig.4, and multi-stage (multiple rotors and stators) shown in Fig. 5 and Fig. 6, [11,12].

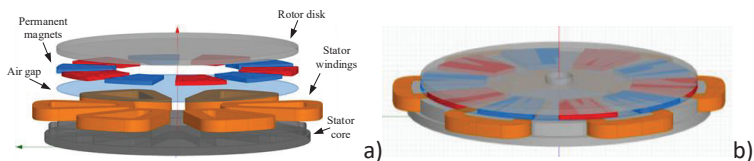


**Figure 1:** Single-sided AFPMG: a) components of the machine, b) model of the machine

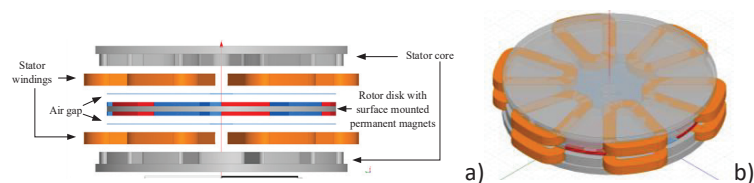


**Figure 2:** Double-sided AFPMG with two external stators and one internal rotor: a) components of the machine, b) model of the machine

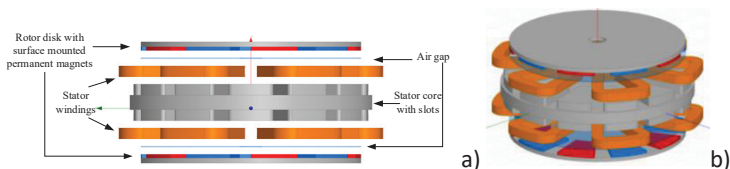


**Figure 3:** Double-sided AFPMG with two external rotors and one internal stator: a) components of the machine, b) model of the machine

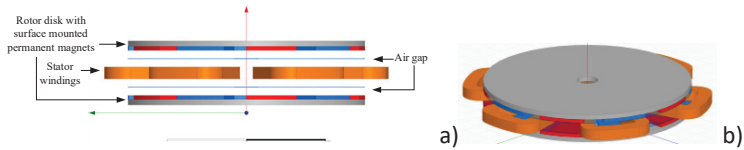


**Figure 4:** Double-sided coreless AFPMM with two external rotors and one internal stator: a) components of the machine, b) model of the machine

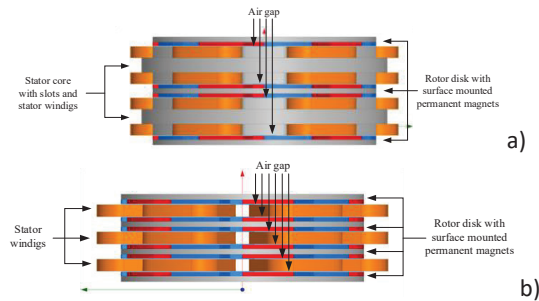


**Figure 5:** Multistage AFPMM: a) with stator cores, b) coreless

This article deals with the coreless double-sided topology with two outer rotor discs with surface-mounted permanent magnets and one inner coreless stator.

Since it is a coreless topology, there is no cogging torque present, [16], and also no stator core losses. Due to the absence of the core losses, these types of generators can operate at higher efficiencies compared to conventional generators, [2-5].

These types of machines can be used for low-speed applications because they usually have a large pole number. Electromagnetic force (EMF) and torque production are mainly limited by:

- limited mass of the machine and its outer dimensions, due to the application of the machine, and
- limited electrical current density, due to the heating of the windings.

The outer dimensions of the machine limit the space for windings, and the permanent magnet (PM) installation and maximum allowed temperature limit the electrical current density in the windings [7,18].

EMF and torque depend on the magnetic flux density in the air gap, namely the axial component of the magnetic flux density in the air gap, which passes between PMs on opposite rotor disks, [22]. This dependency is represented with Faraday's induction law for time changing magnetic field, [36].

Magnetic flux density in the air gap depends on:

- active copper volume, and [19],
- PM volume (determined by PM thickness, pole number and inner and outer radius of the active part of the machine [20]) and
- electrical current density in the windings.

From the text above, it can be concluded that magnetic flux density in the air gap is one of the key values for torque and EMF production, since it is connected to all the machine dimensions and materials, [23,24].

Since this article deals with a coreless machine, a suitable stator thickness must be selected, because it also represents a large air gap for the magnetic flux density, [26]. Suitable stator thickness reduces the magnetic flux leakage from the south to north pole on the same PM (Path 2 in Fig.6).

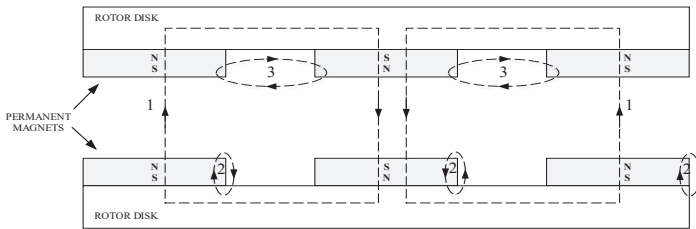


**Figure 6:** Sectional view of AFPMM with magnetic flux paths

Magnetic flux leakage between neighbouring PMs (Path 3 in Fig. 6) can be reduced with a suitable distance between them, [27]. It must be considered that suitable stator thickness also influences the magnetic flux leakage presented as Path 3, and the angle of PMs influences the magnetic flux leakage presented with Path 2.

Many design methodologies for AFPMM are connected to simple design equations, [20, 28, 29], used for preliminary design. Analytical methods offer a fast preview of torque production of the machine with a certain degree of accuracy, [30]. The finite element method (FEM) is an accurate numerical method and requires much time for simulations, [16, 20, 31-33, 35]. Recent works deal with solving this problem by developing different analytical methods, which require certain simplifications and assumptions, [17], that influence the accuracy of the results but offer a faster determination of magnetic flux density in an explicit form, [45]. Derivation of equations for magnetic flux density calculation from Maxwell’s equations is a commonly used approach, [35].

This article presents a methodology for designing coreless AFPMM through using a polynomial for magnetic flux density calculation, which was determined by using the least square approximation (LSA) method.

Combining the polynomial and a well-known analytical equation for torque calculation, a new equation for the torque calculation of an AFPMM is determined for various stator thicknesses.

Torque was calculated for different stator thicknesses using the new equation and compared with the results of FEM analysis.

## 2 METHODOLOGY

### 2.1 Simplified FEM

The axial component of magnetic flux density in the middle of the stator was determined by a simplified finite element method (FEM) for different stator thicknesses of a double-sided coreless AFPMM.

The simplification of the FEM calculations is the use of the air between the rotor disks instead of the stator with its windings, which is possible due to the similarity of permeability of air and copper. The tool used was the Ansys Maxwell 3D software. The values of the axial component of the magnetic flux density in the middle of the stator (air) were obtained on a centreline between two permanent magnets for various stator thicknesses by using an LSA method, resulting in a polynomial for calculating the axial component of magnetic flux density in the middle of the stator for different stator thicknesses.

EMF and torque were calculated for different stator thicknesses and compared with the results of FEM analysis and measurements of the prototype machine.

A 3D model of the generator was constructed, which is based on an actual prototype, presented in [36]. Its data are presented in Table 1. These dimensions were chosen for easier verification of the results with actual laboratory measurements.

**Table 1:** Geometry and parameters of analysed AFPMM, [36]

Symbol	Quantity	Value/Unit
$R$	Rotor disk radius	150 mm
$d_{Fe}$	Rotor disk thickness	7 mm
$d_m$	Permanent magnet thickness (NdFeB)	5 mm
$\tau_m$	Magnetic pitch	25°
$D_i$	Inner diameter of PM	80 mm
$D_o$	Outer diameter of PM	150 mm
$B_r$	Remnant magnetic flux density	1.22 T
$\tau_p$	Pole pitch	36°
$I$	Electrical current	2x10 A
	Number of windings	6
$d_s$	Winding thickness	15 mm
$d_c$	Coil width	20 mm
$S_w$	Copper wire cross section	1.23 mm <sup>2</sup>
$d_{ag}$	Air gap thickness	1 mm
$m$	Number of phases	3
$k_w$	Winding factor	0.966
$p$	Number of pole pairs	5

For different stator thicknesses, simplified FEM calculations were performed, based on which, the axial component of magnetic flux density was analysed on a centreline between the PMs on the opposite rotor disks. The position of the centreline and the dimensions of the PMs are shown in Fig. 7.

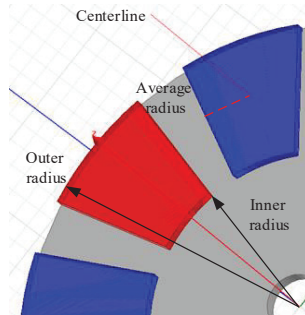


**Figure 7:** Dimensions of the PMs and the centreline

Fig. 8 shows the meshed model of rotor disks with surface mounted PMs with a 55 mm fictitious air gap between them, which represents the thickness of the stator and both air gaps.

The middle of the distance between PMs on the opposite rotor disks also represents the the middle of the stator. Values of the axial component of the magnetic flux density were used to determine the polynomial for the calculation of magnetic flux density in the middle of the stator for different stator thicknesses.

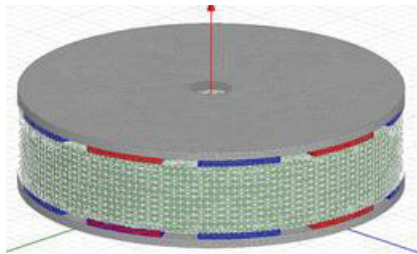


**Figure 8:** Meshed AFPMM model with 55 mm fictitious air gap

Fig. 9 shows a single value waveform for a 55 mm distance between PMs on opposite rotor disks (marked as a fictitious air gap) and the magnetic flux density values near the PM and in the middle of the stator, respectively marked as  $B_{z\_max}$  and  $B_{z\_min}$ .

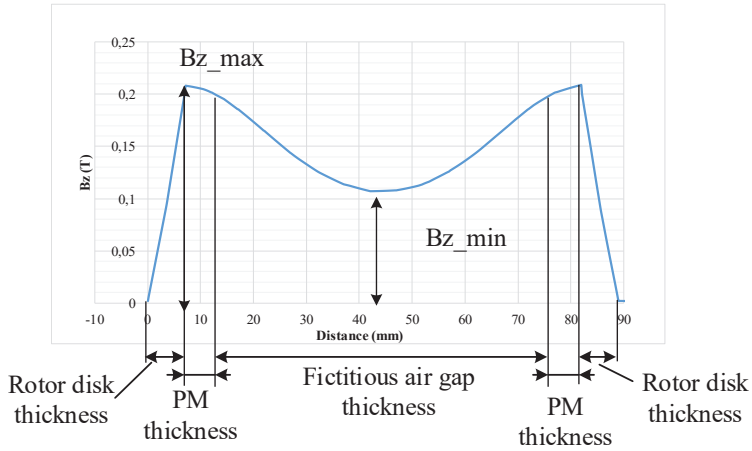


Figure 9: Positions of maximum and minimum axial component magnetic flux density

## 2.2 Least square approximation method

Values for  $B_{z\_min}$  were used to produce a polynomial using an LSA method, which is a mathematical procedure that can find a curve that best fits a known set of given points by minimizing the sum of the squares of the offsets (“the residuals”) of the points from the curve. The sum of the squares of the offsets is used instead of the absolute offset values because this allows the residuals to be treated as a continuous differentiable quantity, [37]. Vertical least-squares fitting proceeds by finding the sum of the squares of the vertical deviations  $R^2$  of a set of  $n$  data points, [37], which is presented in (2.1).

$$R^2 \equiv \sum_{i=1}^n \left[ y_i - f(x_i, a_1, a_2, \dots, a_n) \right]^2 \quad (2.1)$$

where  $R$  is the residual,  $y_i$  FEM calculated data point,  $f$  fitting function,  $x_i$  independent variable of fitting function,  $a_1, a_2, \dots$  and are coefficients of fitting function. In the present case the polynomial is chosen as a fitting function.

The condition for  $R^2$  to be a minimum is that for  $i=1, \dots, n$ , the derivative of  $R^2$  equals 0

$$\left( \frac{\partial R^2}{\partial a_i} = 0 \right).$$

As an example, if we use the linear fit (polynomial of first order)  $f(a,b)=a+bx$ , we obtain the following set of equations (2.2), [38].

$$\begin{aligned}
 R^2(a,b) &\equiv \sum_{i=1}^n [y_i - (a+bx_i)]^2 \\
 \frac{\partial(R^2)}{\partial a} &= -2 \sum_{i=1}^n [y_i - (a+bx_i)] = 0 \\
 \frac{\partial(R^2)}{\partial b} &= -2 \sum_{i=1}^n [y_i - (a+bx_i)]x_i = 0
 \end{aligned}
 \tag{2.2}$$

Using the procedure described above and a set of data points for  $B_{z\_min}$ , a polynomial was determined. The analysis is carried out in the middle of the stator because the magnetic flux density is the lowest and presents the safe side in the design of the machine.

### 3 DESIGN OF AN AFPMM WITH LEAST SQUARE APPROXIMATION METHOD

The process of designing AFPMM machines as well as any other form of machine has steps, the first of which is defined by different limitations, such as required torque size, rotation speed, maximum allowed dimensions, etc. Therefore, the starting dimensions of the machine must be estimated with the highest possible accuracy, especially the inner and outer diameters of the PMs and axial length of the machine. A standard approach for determining these dimensions is the use of sizing equations, [39, 40].

Two types of sizing equations for AFPMM can be found in the literature. [41]. Equation (3.1) includes (besides electrical and magnetic parameters) inner radius, outer radius and axial length of the machine, [42].

$$P_i = \eta \frac{m}{T} \int_0^T e(t) i(t) dt = \eta m K_p E_{pk} I_{pk}
 \tag{3.1}$$

where  $i(t)$  is phase electrical current,  $m$  number of phases,  $e(t)$  electromagnetic force (EMF),  $\eta$  efficiency of the machine,  $K_p$  electrical power waveform,  $T$  one period of EMF and  $E_{pk}$  and  $I_{pk}$  peak values of EMF and phase current [42].

This article deals with the second type of sizing equations, so the elements of (3.1) are not described in detail.

The second type of sizing equation (3.2) includes the connection between electromagnetic torque and basic geometrical, electrical and magnetic parameters.

$$T_{em} = \frac{\pi}{4} B_z A_{in} K_d \lambda (1 - \lambda^2) D_o^3
 \tag{3.2}$$

where  $T_{em}$  is the electromagnetic torque,  $A$  electrical current density and  $K_d$  flux leakage factor,  $\lambda$  ratio between the inner and outer diameter of the PMs,  $D_o$  outer diameter of the PM [44]. Considering the line current density, Equation (3.2) can be written as (3.3)

$$T_{em} = \frac{1}{4} \alpha_i m I N k_w B_z (D_o^2 - D_i^2) \quad (3.3)$$

where  $\alpha_i$  is the angle of PMs divided by the pole angle,  $m$  number of phases,  $I$  electrical current,  $k_w$  winging factor,  $N$  number of turns per coil,  $B_z$  axial component of magnetic flux density and  $D_o$  and  $D_i$  outer and inner PM diameter respectively.

By inserting the polynomial for determining the axial component of magnetic flux density in the middle of the fictitious air gap into equation (3.3), a new equation emerges for electromagnetic torque calculation that considers different stator thicknesses.

## 4 RESULTS

Simplified FEM was used to produce a set of data points for  $B_{z\_min}$  and  $B_{z\_max}$  for the AFPMM described in Table 1. Fig. 10 and Table 2 show that the maximum and minimum values of  $B_z$  are very close up to the 25mm fictitious air gap thickness.

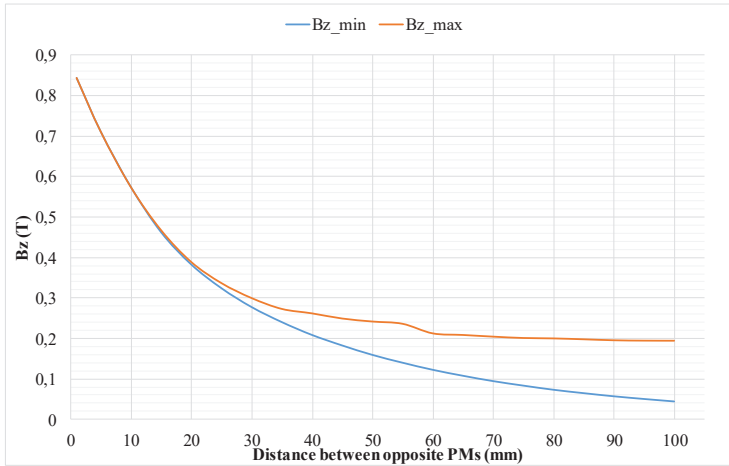


Figure 10:  $B_{z\_max}$  and  $B_{z\_min}$  in axial direction between the PMs

**Table 2:** Axial component of magnetic flux density in the fictitious air gap (simplified FEM)

Distance between opposite PMs $d$ (mm)	$B_{z\_min}$ (T)	$B_{z\_max}$ (T)	Difference (%)
1	0.8448	0.8448	0
5	0.7118	0.7118	0
10	0.5745	0.5745	0
15	0.4628	0.4682	1.15
20	0.3828	0.3895	1.71
25	0.3241	0.3373	3.94

Using the LSA and data from Table 2, a polynomial (4.1) was determined for the axial component of magnetic flux density in the middle of the stator for different stator thicknesses.

$$B_z = 0,883941142648657 - 0,038685876107852 \cdot d + 0,000823824267761 \cdot d^2 - 0,000006968242777 \cdot d^3 \tag{4.1}$$

where  $B_z$  is the axial component of magnetic flux density in the middle of the fictitious air gap and  $d$  the thickness of the fictitious air gap. By inserting (4.1) into (3.3), a new equation (4.2) emerges for electromagnetic torque calculation that considers different stator thicknesses.

$$T_{em} = \frac{1}{4} \alpha_1 m I N k_w \left( \begin{matrix} 0,8839 - \\ 0,0387 \cdot d + \\ 0,8238 \cdot 10^{-3} \cdot d^2 - \\ 0,6968 \cdot 10^{-5} \cdot d^3 \end{matrix} \right) (D_o^2 - D_i^2) \tag{4.2}$$

We have derived a new polynomial for calculating the axial component of magnetic flux density in the middle of the stator for different stator thicknesses for the maximum of 25 mm stator thickness together with air gaps on both sides, because the results in Table 2 show the acceptable deviation of 3.94% at fictitious air gap 25 mm.

### 4.1 Verification of results

Equation (4.2) represents a new equation for AFPMM electromagnetic torque calculation for optimal stator thicknesses. Verification of the electromagnetic torque calculation is performed by comparing the calculated results, gained by using equation (4.2), and the results gained by FEM simulations of the AFPMM described in Table 1.

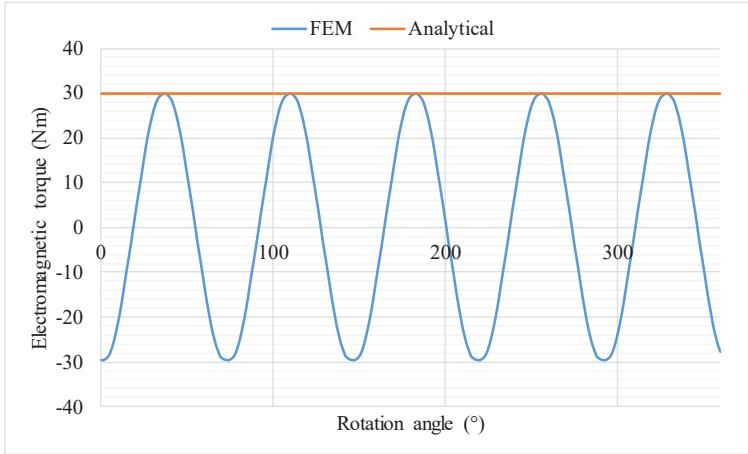


**Figure 11:** Comparison of FEM and analytically calculated electromagnetic torque

Fig. 11 shows the calculated electromechanical (static) torque gained by using equation (4.2) and FEM. The result gained by equation (7) is 29.82 Nm and 29.78 Nm by FEM, which means that there is only 0.15% difference.

FEM and analytically calculated results are also compared to the results of measurements of the actual prototype. Measurement results are reported in [43], and for 600 rpm rotational speed electromechanical torque of 29.4 Nm was measured. Calculated results are in good agreement with the measured value: the difference between them is less than 1.5%.

Additional FEM analysis were performed for 3 stator thicknesses (5, 10, and 20 mm). Fig. 12 shows the comparison of results.

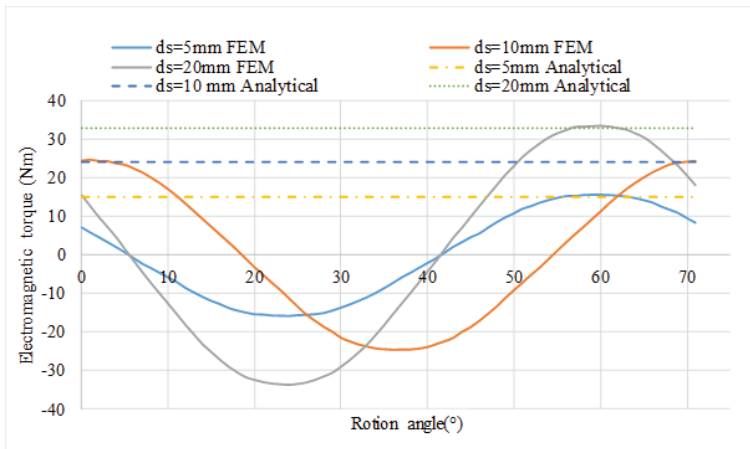


**Figure 12:** Comparison of FEM and analytically calculated electromagnetic torque for different stator thicknesses

Matching between the FEM and analytically calculated torque for 5 mm stator thickness is 96.5%, 98.06% for 10 mm stator thickness, and 98.34% for 20 mm stator thickness

## 5 CONCLUSION

This article presents a methodology for designing AFPMM, especially in the preliminary stage. Once the initial geometrical parameters are determined, a few simplified FEM calculations combined with LSA can produce a polynomial that offers a fast preview of the EMF and torque production of the machine for different stator thicknesses. Agreement between the results obtained via FEM, the analytically calculated results, and measured results for one stator thickness confirms that the presented methodology offers quite accurate results.

## References

- [1] **F. Danang Wijaya, N. A. Rahadyan, and H. R. Ali**, "Magnetic flux distribution due to the effect of stator-rotor configuration in the axial machine," Proc. - 2014 6th Int. Conf. Inf. Technol. Electr. Eng. Leveraging Res. Technol. Through Univ. Collab. ICITEE 2014, no. d, 2015.
- [2] **S. Ekram**, "A novel windmill generator," Proc. - 12th Int. Conf. Electr. Mach. Syst. ICEMS 2009, 2009.
- [3] **A. Pop, F. Gillon, and M. M. Radulescu**, "Modeling and permanent-magnet shape optimization of an axial-flux machine," Proc. - 2012 20th Int. Conf. Electr. Mach. ICEM 2012, no. c, pp. 357–363, 2012.
- [4] **Y. Cao, L. Yu and H. Jia**, "Rotor mechanical stress and deformation analysis of coreless stator axial-flux permanent magnet machines," *2015 IEEE Magnetics Conference (INTERMAG)*, Beijing, 2015, pp. 1-1.
- [5] **X. Wei and K. Yang**, "Research of stator displacement technique in multi-stage axial-flux permanent magnet machines," *2015 IEEE Magnetics Conference (INTERMAG)*, Beijing, 2015, pp. 1-1.
- [6] **F. Caricchi, F. Crescimbin, F. Mezzetti, and E. Santini**, "Multi-stage axial-flux pm machine for wheel direct drive," *IEEE Trans. Ind. Appl.*, vol. 32, no. 4, pp. 882–888, 1996.
- [7] **A. Daghigh, H. Javadi and H. Torkaman**, "Improved design of coreless axial flux permanent magnet synchronous generator with low active material cost," *The 6th Power Electronics, Drive Systems & Technologies Conference (PEDSTC2015)*, Tehran, 2015, pp. 532-537.
- [8] **L. Drazikowski and W. Koczara**, "Permanent magnet disk generator with coreless windings," *COMPEL Int. J. Comput. Math. Electr. Electron. Eng.*, vol. 31, no. 1, pp. 108–118, 2012.
- [9] **A. Hemeida, P. Sergeant, A. Rasekh, H. Vansompel and J. Vierendeels**, "An optimal design of a 5MW AFPMSM for wind turbine applications using analytical model," *2016 XXII International Conference on Electrical Machines (ICEM)*, Lausanne, 2016, pp. 1290-1297.
- [10] **M. Aydin, M. Gulec, Y. Demir, B. Akyuz, and E. Yolacan**, "Design and validation of a 24-pole coreless axial flux permanent magnet motor for a solar powered vehicle," *2016 XXII Int. Conf. Electr. Mach.*, pp. 1493–1498, 2016.

- [11] **N. Takorabet, J. P. Martin, F. Meibody-Tabar**, F. Sharif, and P. Fontaine, "Design and optimization of a permanent magnet axial flux wheel motors for electric vehicle," Proc. - 2012 20th Int. Conf. Electr. Mach. ICEM 2012, no. c, pp. 2635–2640, 2012.
- [12] **R.-B. Mignot, F. Dubas, C. Espanet, and E. D. Chamagne**, "Design of axial flux PM motor for electric vehicle via a magnetic equivalent circuit," 2012 First Int. Conf. Renew. Energies Veh. Technol., pp. 212–217, 2012.
- [13] **N. Takorabet, J. P. Martin, F. Meibody-Tabar, F. Sharif and P. Fontaine**, "Design and optimization of a permanent magnet axial flux wheel motors for electric vehicle," 2012 XXth International Conference on Electrical Machines, Marseille, 2012, pp. 2635-2640.
- [14] **T.-U. Jung**, "Electromagnetic design analysis and performance improvement of axial field permanent magnet generator for small wind turbine," J. Appl. Phys., vol. 111, no. 7, p. 07E708, 2012.
- [15] **G. J. Yan, L. Y. Hsu, J. H. Wang, M. C. Tsai, and X. Y. Wu**, "Axial-flux permanent magnet brushless motor for slim vortex pumps," IEEE Trans. Magn., vol. 45, no. 10, pp. 4732–4735, 2009.
- [16] **F. Giulii Capponi, G. De Donato, and F. Caricchi**, "Recent advances in axial-flux permanent-magnet machine technology," IEEE Trans. Ind. Appl., vol. 48, no. 6, pp. 2190–2205, 2012.
- [17] **Z. Shabahang, M. Shahnazari and A. Sedighi**, "Analysis of dynamic eccentricity in a coreless axial flux permanent magnet machine," 2015 30th International Power System Conference (PSC), Tehran, 2015, pp. 358-362.
- [18] **Chen, R. Nilssen, and A. Nysveen**, "Performance comparisons among radial flux, multi-stage axial flux and three-phase transverse flux pm machines for downhole applications," 2009 IEEE Int. Electr. Mach. Drives Conf. IEMDC '09, pp. 1010–1017, 2009.
- [19] **Hanselman, D.**: Brushless permanent magnet motor design, Magna Physics Pub., USA, 2006.
- [20] **Gieras, J.F., Wang, R.J., Kamper M.J.**, Axial Flux Permanent Magnet Brushless Machines, Kluwer Academic Publishers, Dordrecht, 2004.
- [21] **S. Lomheim**, "Analysis of a Novel Coil Design for Axial Flux Machines," M.S. Thesis, Norwegian University of Science and Technology, Department of Electric Power Engineering, Jun. 2013.
- [22] **W. Jara, A. Martin, and J. A. Tapia**, "Axial flux PM machine for low wind power generation," 19th Int. Conf. Electr. Mach. ICEM 2010, 2010.
- [23] **Daghigh, H. Javadi, and A. Javadi**, "Improved Analytical Modeling of Permanent Magnet Leakage Flux in Design of the Coreless Axial Flux Permanent Magnet Generatorx," Can. J. Electr. Comput. Eng., vol. 40, no. 1, pp. 3–11, 2017.
- [24] **Caricchi, F. Crescimbin, O. Honorzti, G. Lo Bianco and E. Santini**, "Performance of coreless-winding axial-flux permanent-magnet generator with power output at 400 Hz-3000 rev/min," *Industry Applications Conference, 1997. Thirty-Second IAS Annual Meeting, IAS' 97., Conference Record of the 1997 IEEE*, New Orleans, LA, 1997, pp. 61-66 vol.1.

- [25] **M. Sadeghierad, H. Lesani, H. Monsef and A. Darabi**, "Leakage flux consideration in modeling of high speed axial flux PM generator," *2008 IEEE International Conference on Industrial Technology*, Chengdu, 2008, pp. 1-6.
- [26] **Lee, K. Jeon, Y. Kim and S. Jung**, "Performance evaluation of coreless axial flux permanent magnet wind generator," *2015 IEEE Magnetics Conference (INTERMAG)*, Beijing, 2015, pp. 1-1.
- [27] **Mbidi, David Natangue**, "Design and Evaluation of a 300 kW Double Stage Axial-Flux Permanent Magnet Generator," M.S. Thesis, Stellenbosch University, 2001.
- [28] **S. Kahourzade, A. Mahmoudi, N. A. Rahim, and H. W. Ping**, "Sizing equation and finite element analysis optimum design of axial-flux permanent-magnet motor for electric vehicle direct drive," *2012 IEEE Int. Power Eng. Optim. Conf. PEOCO 2012 - Conf. Proc.*, no. June, pp. 1–6, 2012.
- [29] **V. Rallabandi, N. Taran, D. M. Ionel, and J. F. Eastham**, "On the feasibility of carbon nanotube windings for electrical machines - Case study for a coreless axial flux motor," *ECCE 2016 - IEEE Energy Convers. Congr. Expo. Proc.*, 2017.
- [30] **Y. Wang, W. X. C. Chen, and Z. Dong**, "A parametric magnetic network model for axial flux permanent magnet machine with coreless stator," *2014 17th Int. Conf. Electr. Mach. Syst. ICEMS 2014*, pp. 1108–1113, 2015.
- [31] **J. M. Seo, I. S. Jung, H. K. Jung and J. S. Ro**, "Analysis of Overhang Effect for a Surface-Mounted Permanent Magnet Machine Using a Lumped Magnetic Circuit Model," in *IEEE Transactions on Magnetics*, vol. 50, no. 5, pp. 1-7, May 2014.
- [32] **A. Mahmoudi, N. a. Rahim, and W. P. Hew**, "Axial-flux permanent-magnet machine modeling, design, simulation and analysis," *Sci. Res. Essays*, vol. 6, no. 12, pp. 2525–2549, 2011.
- [33] **N. Taran and M. Ardebili**, "A novel approach for efficiency and power density optimization of an Axial Flux Permanent Magnet generator through genetic algorithm and finite element analysis," *2014 IEEE 23rd International Symposium on Industrial Electronics (ISIE)*, Istanbul, 2014, pp. 709-714.
- [34] **J. Azzouzi, G. Barakat, and B. Dakyo**, "Quasi-3D analytical modeling of the magnetic field of an axial flux permanent magnet synchronous machine," *Electr. Mach. Drives Conf. 2003. IEMDC'03. IEEE Int.*, vol. 3, no. 4, pp. 1941–1947 vol.3, 2003.
- [35] **P. Vrtic, P. Pisek, T. Marcic, M. Hadziselimovic and B. Stumberger**, "Analytical Analysis of Magnetic Field and Back Electromotive Force Calculation of an Axial-Flux Permanent Magnet Synchronous Generator With Coreless Stator," in *IEEE Transactions on Magnetics*, vol. 44, no. 11, pp. 4333-4336, Nov. 2008.
- [36] **P. Vrtic, M. Vrazic and G. Papa**, "Design of an Axial Flux Permanent Magnet Synchronous Machine Using Analytical Method and Evolutionary Optimization," in *IEEE Transactions on Energy Conversion*, vol. 31, no. 1, pp. 150-158, March 2016.
- [37] **Weisstein, Eric W.** "Least Squares Fitting." From MathWorld--A Wolfram Web Resource. <http://mathworld.wolfram.com/LeastSquaresFitting.html>

- [38] **Kenney, J. F. and Keeping, E. S.** “Linear Regression and Correlation.” Ch. 15 in *Mathematics of Statistics*, Pt. 1, 3rd ed. Princeton, NJ: Van Nostrand, pp. 252–285, 1962.
- [39] **A. Chen, R. Nilssen, and A. Nysveen,** “Performance comparisons among radial-flux, multi-stage axial-flux, and three-phase transverse-flux PM machines for downhole applications,” *IEEE Trans. Ind. Appl.*, vol. 46, no. 2, pp. 779–789, Apr. 2010.
- [40] **O. Kalender, Y. Ege, and S. Nazlibilek,** “Design and determination of stator geometry for axial flux permanent magnet free rod rotor synchronous motor,” *Measurement*, vol. 44, no. 9, pp. 1753–1760, 2011.
- [41] **J. Pyrhönen, T. Jokinen, and V. Hrabovcová,** *Design of Rotating Machines*, Chichester, U.K.: Wiley, 2009.
- [42] **S. Huang, J. L. F. Leonardi, and T. A. Lipo,** “A comparison of power density for axial flux machines based on general purpose sizing equations,” *IEEE Trans. Energy Convers.*, vol. 14, no. 2, pp. 185–192, Jun. 1999.
- [43] **P. Vrtič,** “Načrtovanje in analiza sinhronskih strojev s trajnimi magneti in aksialnim magnetnim pretokom,” Doctoral thesis, University of Maribor, Maribor, 2008.
- [44] **E. Spooner and B. J. Chalmers,** ““TORUS”: A slotless, toroidal-stator, permanent-magnet generator,” *Proc. Inst. Elect. Eng.—Elect. Power Appl.*, vol. 139, no. 6, pp. 497–506, Nov. 1992.

## Nomenclature

(Symbols)	(Symbol meaning)
$R$	rotor disk radius
$d_{Fe}$	rotor disk thickness
$d_M$	permanent magnet thickness
$\tau_m$	magnetic pitch
$D_i$	inner radius of PM
$D_o$	outer radius of PM
$B_r$	remnant magnetic flux density
$\tau_p$	pole pitch
$p$	number of pole pairs
$I$	rated phase current
$i(t)$	phase electrical current,
$e(t)$	electromagnetic force
$\eta$	efficiency of the machine
$K_p$	electrical power waveform
$K_d$	flux leakage factor

---

$T$	one period of EMF
$E_{pk}$	peak value of EMF
$I_{pk}$	peak value of phase current
$B_{z\_max}$	magnetic flux density near the PM
$B_{z\_min}$	magnetic flux density in the middle of the stator
$R$	Residual in LSA
$y_i$	FEM calculated data point
$f$	fitting function
$x_i$	independent variable of fitting function
$a_1, a_2$	fitting function coefficients
$A$	electrical current density
$T_{em}$	electromagnetic torque
$\lambda$	ratio between inner and outer diameter of the PMs
$\alpha_i$	angle of PMs divided with the pole angle
$B_z$	axial component of magnetic flux density
$d$	thickness of the fictitious air gap
$N$	number of turns per coil
$d_c$	coil width
$d_s$	stator thickness
$m$	number of phases
$d_{ag}$	air-gap thickness
$S_w$	Copper wire cross-section
$k_w$	winding factor

# IMPROVING DECENTRALIZED ECONOMIC GROWTH AND REDUCING ENERGY CONSUMPTION IN THE EUROPEAN UNION WITH THE APPLICATION OF ECOLOGICALLY ORIENTED INNOVATIONS

## IZBOLJŠANJE DECENTRALIZIRANE GOSPODARSKE RASTI V EVROPSKI UNIJI IN ZMANJŠEVANJE RABE ENERGIJE Z UPORABO EKOLOŠKO NARAVNANIH INOVACIJ

Niko Natek<sup>33</sup>, Boštjan Krajnc

**Keywords:** Energy efficiency, Ecology, Innovation, Economy, waste-water treatment, constructed wetlands, green-house gas emissions, EU

### **Abstract**

This article presents applicable approaches for supporting the transition towards sustainable decentralized economic development within the European Union, based on the concept of supporting the development and market uptake of eco-innovations. The main topic addressed is achieving a more effective market uptake of ecologically oriented innovations facilitated through matchmaking, as well as knowledge and technology transfer between key actors of the innovation process.

<sup>33</sup> Corresponding author: Niko Natek, Tel.: +386 3 896 1520, Fax: +386 3 896 1522, Mailing address: KSSENA - Energy Agency of Savinjska, Šaleška and Koroška Region, Titov trg 1, 3320 Velenje, Slovenija  
E-mail address: [niko.natek@kssena.velenje.eu](mailto:niko.natek@kssena.velenje.eu)

## **Povzetek**

Članek predstavlja izvedljive pristope za podporo tranzicije v smeri trajnostnega in decentraliziranega razvoja gospodarstev Evropske unije na podlagi uporabe koncepta podpore razvoja in tržne implementacije eko-inovacij. Glavna obravnavana tema je možnost doseganja bolj učinkovitega tržnega preboja ekološko usmerjenih inovacij spodbujenega z aplikacijo povezovanja ter prenosa znanja in tehnologije med ključnimi igralci inovacijskega procesa.

## **1 INTRODUCTION**

National economies within the European Union are vastly divergent in terms of current development, specific problematic areas, and future priorities. In particular, economies from the south-eastern part of Europe are significantly limited in terms of access to resources (human resources as well as critical raw materials and capital) required to fuel future growth, which is a prerequisite to maintaining stability in the context of future economic cohesion that is strongly dependent on maintaining a high growth rate of GDP. Promoting decentralized growth across the EU has been one of the main principles of European integration but has not been adequately implemented so as to achieve an equilibrium of development in key areas such as education, business and employment (preferably in knowledge-intensive industries) in each of these countries. A clear indicator of this mismatch is illustrated in the extensive outflux of human capital from poorer countries to highly developed economies offering better opportunities for gainful employment and career development. The donor countries providing human capital through domestic investment into formal education are left without skilled labour that could raise the development level of their national economies, further exacerbating the prosperity gap within the EU. Nonetheless, the shift from conventional industries towards sustainable economies offers opportunities for less privileged countries to begin anew with ample opportunities to redesign national economies by comprehensively addressing development from a bottom-up approach, drawing from basic and applied research.

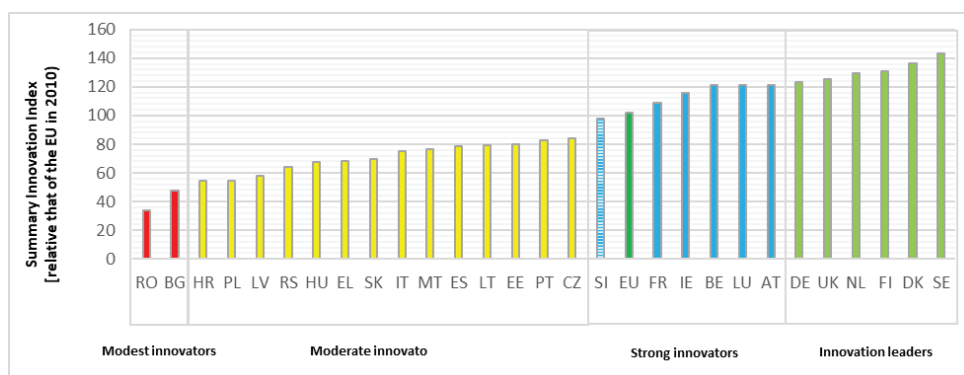


**Figure 1:** Performance in innovation by country, [1]

The future development and large-scale implementation of novel energy technologies open a plethora of market niches where less developed markets have somewhat of an advantage over highly developed ones. In terms of future ambitions of the region to build its energy sector on the basis of efficient use of energy, a high share of (intermittent) renewable energy sources with hydrogen accompanying electricity as the key vector for transport and storage of energy, it is essential to focus on activities that will enable the research and production of required equipment and infrastructure domestically to the highest possible extent.

## 2 ECO-INNOVATION

Eco-innovation is defined as the innovative creation and commercialization of new environmental technologies, products, and services that reduce the overall negative environmental impact and enable the co-creation of viable and sustainable solutions targeting specific environmental issues. As such, the concept addresses all the key challenges that societies within the European Union and beyond will have to overcome in the coming decades and shows a clear way forward for companies, decision-makers, educational institutions and academia, research and development organizations as well as the general public in the role of final consumers and beneficiaries. Implementing support measures for eco-innovation on a systemic level, be it policy adaptation, entrepreneurial development, educational reform, energy transition and so forth, will be essential in achieving inclusive, robust, and sustainable growth over the long term. This process will have to be all-encompassing to engage and facilitate requirements of literally all types of institutions and individuals, from legislative to judiciary and executive branches of government, research and educational institutions to companies, from producers to consumers.



*Figure 2: Ecolnn Danube project logo, [1]*

Creating a better environment for enterprise, innovation and the citizens in general, while prioritizing sustainable development will, among other things, require increasing the level of awareness among final consumers, improving the quality of obtained skills amongst the regions human resource pool as well as creating market opportunities in areas crucial to the future wellbeing of the societies in the wider region (ecology-environmental protection, waste/resource management, energy supply, transport, etc.). A swifter move towards the new economic model of a circular economy enables the decoupling of economic growth from negative environmental effects, decreasing energy and resource dependency of the region, reducing labour intensity by increasing labour productivity and prioritizing industries that demonstrate high value-added and long-term sustainability, not only from an economic point of view but based on the complete life cycle impact, taking into account the wider benefits that it implies for the society as a whole.

Achieving a practical implementation of such an economic model will require substantial effort and engagement of various stakeholders across all levels, focusing in particular on the interconnectivity amongst relevant actors as well as to increase the flow of information and knowledge across transnational channels within the European Union.

### 3 VIRTUAL LAB STAKEHOLDER PLATFORM

The EcoInn Danube project (Eco-innovatively connected Danube Region) was structured on the primary premise that achieving wider market uptake of innovations with notable positive ecological impact can be achieved through the facilitation of cooperation between key innovation actors from various types of institutions by applying the quadruple helix approach. The development of new interactions and the strengthening of existing interactions amongst representatives of the eco-innovation environment was recognized as the most effective approach to increase the supply and demand of eco-innovative products by means of improving transnational cooperation on the markets of the countries within the Danube region, the EU, and in a global context.

The project addressed the challenges in a comprehensive approach that was derived from preliminary results of extensive analytical and research activities inclusive of current country-specific status with regard to obstacles and opportunities, existing support structures, analysis of political, economic, social, technological, environmental, legal considerations and so forth. The core activities of the project were however focused on direct matchmaking of key stakeholder groups, implemented through various types of events (green summer schools, green innovation forums, local/national and international stakeholder meetings, local workshops and information events, etc.) as well as through the provision of novel IT tools.

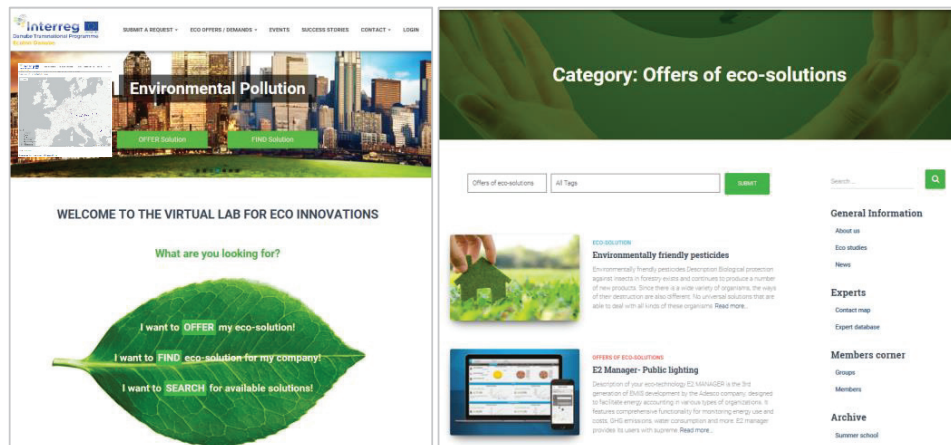


Figure 3: Virtual lab web platform, [1]

One of the main tools developed in this regard was the virtual lab platform, with a key function to provide a matchmaking portal for pairing offers and demands of eco-innovations. The virtual lab achieved a notable input from individuals (independent innovators, students), research and academic institutions as well as companies regarding specific eco-innovative products and services developed by said organizations. The final development of the virtual lab was the

organization of an international competition, in which the most promising eco-innovations with respect to predefined criteria were chosen, for which comprehensive feasibility studies of their developed products and/or services will be developed. One of the three best overall products chosen was an innovative design of a constructed wetland for treating municipal waste-water.

## **4 LOW-ENERGY CONSUMPTION WASTEWATER TREATMENT METHODS**

Water as a compound is relatively abundant as it covers roughly 71% of the Earth's surface. The total water reserves represent roughly 0.02% of the planet's mass which would amount to about  $1.35 \times 10^{18}$  metric tonnes or 1.386 billion cubic kilometres ( $\text{km}^3$ ) as volume, [1]. However, the majority of water reserves are not made available in a form that is economically/technically appropriate for human consumption. The vast majority is salt-water of which 96.5% is contained within oceans and about 1% below ground. Freshwater reserves represent roughly 2.5%, of which 70% is ice. Merely 1.3% is freshwater, mostly located inside lakes. Generally, only groundwater (0.4%) and surface water (0.004%) are viable sources for human consumption, indicating that water reserves are considerably scarce in practical terms. The water cycle in itself is a cleaning mechanism, which allowed the reuse of water reserves throughout aeons. In essence, it could be concluded that all previous generations of human beings drank and used the very "same" water.

However, never before in history has the impact of human existence on water reserves been so profoundly negative and so extensive in scope, that natural cleaning mechanism cannot keep pace with ever-growing demand and pollution.

The predominant objective of waste-water treatment is the disposal (management, treatment, reuse) of human-originated and industrial effluents that does not threaten human health and subject the natural environment to undesirable damage. Waste-water treatment is defined as a series or combination of various physical (mechanical), chemical and biological processes and operations applied with the goal of removing pollutants such as solids, organic matter, and nutrients from influent waste-water.

Conventional waste-water treatment is an energy-intensive process. There are over 22,000 waste-water treatment plants in Europe; their operations account for more than 1% of overall electricity consumption within the EU. Annually, the combined final electricity consumption for all the participating plants is over 15 GWh, [2]. Reducing the energy requirements for waste-water treatment would extensively support the efforts of the EU to reduce energy dependency and energy-related emissions. Considering that energy use within the sector could be reduced by a conservative 10%, this would imply a reduction of GHG emission by 4.47 million tonnes of  $\text{CO}_2$  equivalent, [3]. Waste-water treatment, therefore, can be considered one of the many areas that would be optimally addressed comprehensively through the prism of life-cycle assessment and eco-innovation.

### **4.1. Constructed wetlands**

Constructed wetlands are engineered systems that apply natural processes for waste-water treatment. Generally, they are composed by wetland vegetation (macrophyte coverage of varying degree) and filter mediums (soils, sands) placed in separated shallow basins. In most cases, the

flow of waste-water is driven by gravity, while some applications include additional pumping installations if the gradient on the location is not sufficient. The underlying technology was originally developed in the 1950s in Germany (Käthe Seidel, Max Planck Institute) and has since evolved into a viable waste-water treatment technology for various types of waste-water, [4]. Several variations of the technology exist in which free water surface (FWS), horizontal subsurface flow (HSF) and vertical subsurface flow (VSF) wetlands are the basic types. Several studies, however, indicate that improved treatment performance can be achieved by combining different types of constructed wetlands. Most existing hybrid systems are comprised of interchangeable sections of horizontal and vertical filters; however, various types of constructed wetlands could generally be applied (combined) to achieve desired outcomes in terms of treatment efficiency of specific water pollutants. There are several hundreds of conventionally constructed wetlands in operation across Europe today, the majority of which are located in just a few countries; for example, the Czech-Republic is one of the very few countries that have implemented the technology at scale, with about 250 plants active at present. However, most conventional systems have certain shortcomings in terms of low-efficiency in colder climates and inadequate removal of nitrogenous compounds, which have a profoundly adverse impact on aquatic life due to causing oxygen depletion in receiving water biota, [5].

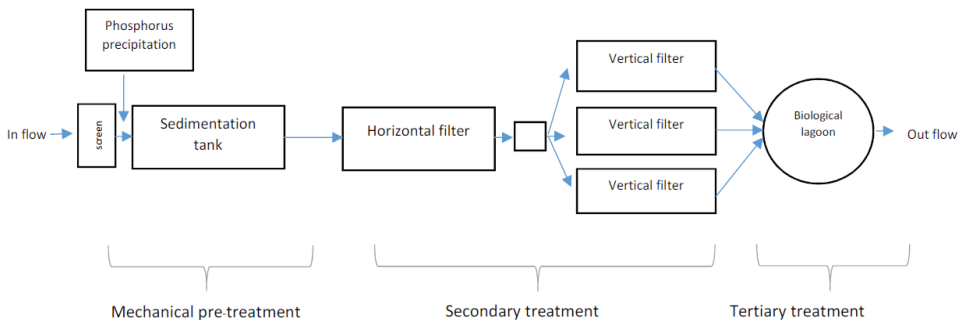


**Figure 4:** Process block scheme (Source: Brno University of Technology)

A team of researchers at the Institute of Landscape Water Management of the Faculty of Civil Engineering at the Brno University of Technology have developed a concept of constructed wetlands that displays a very high efficiency of nitrogen compounds as well as BOD, COD, and TSS removal. The concept has been verified and validated through extensive monitoring of waste-water effluent at a semi-prototype plant located in the village of Dražovice in the Czech Republic. The constructed wetland has undergone a comprehensive reconstruction on one of two horizontal filters with and an improved version of a vertical filter featuring an innovative waste-water dispensing system. The design of the plant allows for comparatively lower capital expenditures within the construction phase against conventional waste-water treatment plants for municipal waste-water; however, the main benefit is its astoundingly low operational costs. The proper design of the plant whereby a sufficient gradient of the landscape on which it is located is available indicates that such a facility does not have any need for energy (or very low requirements in the case that elevation pumps are required) in the secondary stage of waste-water treatment.

## 5 CONCLUSION

Future economic development must take into consideration environmental limitations as primary concerns, especially in the areas of freshwater reserves, sustainable energy supply and critical raw materials. Eco-innovations can offer a competitive edge over industries that still rely on inefficient methods of production, supply and waste management.

Countries of the EU-28 had an energy dependence of 54% (meaning that over one half of its energy needs had to be met by imports) in 2016. Furthermore, a high proportion of said imports, of which about two thirds were represented by petroleum products, gas (24%) and solid fuels (9%), are still concentrated amongst very few exporting partners [6]. The majority of energy imports were provided by Russia, with which the EU has been engaged in an unproductive diplomatic showdown in recent year, exacerbating the associated risks even further.

Eco-innovations that demonstrate very low requirements for critical raw materials, notably reduce the need for energy supply and use of chemicals and even demonstrate a clear economic benefit to the final beneficiary are clearly the way forward. The innovative waste-water system developed by dedicated experts at the Brno University of Technology is just one excellent example of how to address the challenges ahead pragmatically.

## References

- [1] **EcoInn Danube project** (Eco-innovatively connected Danube Region), Interreg Alpine Space transnational programme, 2018
- [2] **Water resources**, information web portal, United States Geological Survey, 2019
- [3] **ENERWATER project** (Continuous assessment, labelling and improvement of overall energy performance of waste-water treatment plants), Horizon 2020, 2018
- [4] **Chang-gyun Lee et al.:** *Nitrogen removal in constructed wetland systems*, Department of Civil Engineering, Monash University, Australia, 2009
- [5] **Jan Vymazal:** *Constructed Wetlands for Wastewater Treatment*, 2010
- [6] **Data viewer on greenhouse gas emissions and removals**, sent by countries to UNFCCC and the EU Greenhouse Gas Monitoring Mechanism (EU Member States), European Environment Agency, 2018





# MAIN TITLE OF THE PAPER SLOVENIAN TITLE

*Author<sup>1</sup>, Author<sup>2</sup>, Corresponding author<sup>✉</sup>*

Keywords: (Up to 10 keywords)

## **Abstract**

Abstract should be up to 500 words long, with no pictures, photos, equations, tables, only text.

## **Povzetek**

(Abstract in Slovenian language)

Submission of Manuscripts: All manuscripts must be submitted in English by e-mail to the editorial office at [jet@um.si](mailto:jet@um.si) to ensure fast processing. Instructions for authors are also available online at <http://www.fe.um.si/en/jet/author-instructions.html>.

Preparation of manuscripts: Manuscripts must be typed in English in prescribed journal form (MS Word editor). A MS Word template is available at the Journal Home page.

A title page consists of the main title in the English and Slovenian language; the author(s) name(s) as well as the address, affiliation, E-mail address, telephone and fax numbers of author(s). Corresponding author must be indicated.

Main title: should be centred and written with capital letters (ARIAL bold 18 pt), in first paragraph in English language, in second paragraph in Slovenian language.

Key words: A list of 3 up to 6 key words is essential for indexing purposes. (CALIBRI 10pt)

Abstract: Abstract should be up to 500 words long, with no pictures, photos, equations, tables, - text only.

Povzetek: - Abstract in Slovenian language.

Main text should be structured logically in chapters, sections and sub-sections. Type of letters is Calibri, 10pt, full justified.

---

✉ Corresponding author: Title, Name and Surname, Organisation, Department, Address, Tel.: +XXX x xxx xxx, E-mail address: x.x@xxx.xx

<sup>1</sup> Organisation, Department, Address

<sup>2</sup> Organisation, Department, Address

Units and abbreviations: Required are SI units. Abbreviations must be given in text when first mentioned.

Proofreading: The proof will be send by e-mail to the corresponding author in MS Word's Track changes function. Corresponding author is required to make their proof corrections with accepting or rejecting the tracked changes in document and answer all open comments of proof reader. The corresponding author is responsible to introduce corrections of data in the paper. The Editors are not responsible for damage or loss of submitted text. Contributors are advised to keep copies of their texts, illustrations and all other materials.

The statements, opinions and data contained in this publication are solely those of the individual authors and not of the publisher and the Editors. Neither the publisher nor the Editors can accept any legal responsibility for errors that could appear during the process.

Copyright: Submissions of a publication article implies transfer of the copyright from the author(s) to the publisher upon acceptance of the paper. Accepted papers become the permanent property of "Journal of Energy Technology". All articles published in this journal are protected by copyright, which covers the exclusive rights to reproduce and distribute the article as well as all translation rights. No material can be published without written permission of the publisher.

Chapter examples:

## 1 MAIN CHAPTER

**(Arial bold, 12pt, after paragraph 6pt space)**

### 1.1 Section

**(Arial bold, 11pt, after paragraph 6pt space)**

#### 1.1.1 Sub-section

**(Arial bold, 10pt, after paragraph 6pt space)**

Example of Equation (lined 2 cm from left margin, equation number in normal brackets (section. equation number), lined right margin, paragraph space 6pt before in after line):

$$\text{Equation} \tag{1.1}$$

Tables should have a legend that includes the title of the table at the top of the table. Each table should be cited in the text.

Table legend example:

***Table 1: Name of the table (centred, on top of the table)***

Figures and images should be labelled sequentially numbered (Arabic numbers) and cited in the text – Fig.1 or Figure 1. The legend should be below the image, picture, photo or drawing.

Figure legend example:

**Figure 1:** *Name of the figure (centred, on bottom of figure, photo, or drawing)*

## References

- [1] **N. Surname:** *Title*, Journal Title, Vol., Iss., p.p., Year of Publication
- [2] **N. Surname:** *Title*, Publisher, Year of Publication
- [3] **N. Surname:** *Title* [online], Publisher or Journal Title, Vol., Iss., p.p., Year of Publication. Available: website (date accessed)

Examples:

- [1] **J. Usenik:** *Mathematical model of the power supply system control*, Journal of Energy Technology, Vol. 2, Iss. 3, p.p. 29 – 46, 2009
- [2] **J. J. DiStefano, A.R. Stubberud, I. J. Williams:** *Theory and Problems of Feedback and Control Systems*, McGraw-Hill Book Company, 1987
- [3] **T. Žagar, L. Kegel:** *Preparation of National programme for SF and RW management taking into account the possible future evolution of ERDO* [online], Journal of Energy Technology, Vol. 9, Iss. 1, p.p. 39 – 50, 2016. Available: [http://www.fe.um.si/images/jet /Volume 9\\_Issue1/03-JET\\_marec\\_2016-PREPARATION\\_OF\\_NATIONAL.pdf](http://www.fe.um.si/images/jet /Volume 9_Issue1/03-JET_marec_2016-PREPARATION_OF_NATIONAL.pdf) (7. 10. 2016)

Example of reference-1 citation: In text [1], text continue.

## Nomenclature

(Symbols)	(Symbol meaning)
<b>t</b>	time

